Constraints on light vector mediators through COHERENT data

Speaker:

Emmanuele Picciau

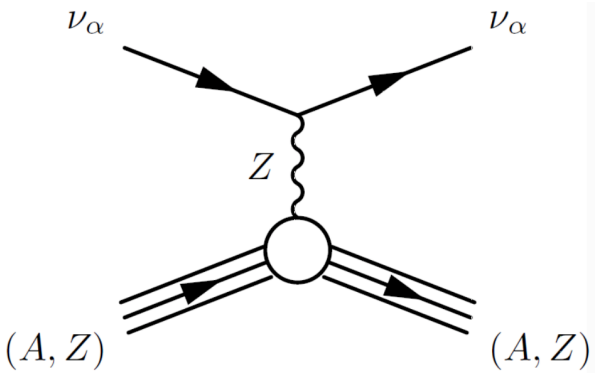

Based on a work in collaboration with

M. Cadeddu
N. Cargioli
F. Dordei
C. Giunti
Y. F. Li
Y. Y. Zhang

Istituto Nazionale di Fisica Nucleare

Constraints on light vector mediators through coherent elastic neutrino nucleus scattering data from COHERENT

M. Cadeddu,[a,b] and N. Cargioli,[b] F. Dordei,[a] C. Giunti,[c] Y.F. Li,[d,e] E. Picciau,[a,b] and Y.Y. Zhang[d,e]

[a] *Istituto Nazionale di Fisica Nucleare (INFN), Sezione di Cagliari, Complesso Universitario di Monserrato - S.P. per Sestu Km 0.700, 09042 Monserrato (Cagliari), Italy*

[b] *Dipartimento di Fisica, Università degli Studi di Cagliari, and INFN, Sezione di Cagliari, Complesso Universitario di Monserrato - S.P. per Sestu Km 0.700, 09042 Monserrato (Cagliari), Italy*

[c] *Istituto Nazionale di Fisica Nucleare (INFN), Sezione di Torino, Via P. Giuria 1, I–10125 Torino, Italy*

[d] *Institute of High Energy Physics, Chinese Academy of Sciences, Beijing 100049, China*

[e] *School of Physical Sciences, University of Chinese Academy of Sciences, Beijing 100049, China*

Reference paper: arXiv:2008.05022 [hep-ph]

Outline of the talk

- Coherent Elastic Neutrino Nucleus Scattering
- Detection of CEvNS by COHERENT collaboration
- Study of light vector mediators using COHERENT data
- Limits on new physics models using COHERENT data

Coherent Elastic Neutrino Nucleus Scattering

PHYSICAL REVIEW D VOLUME 9, NUMBER 5 1 MARCH 1974

Coherent effects of a weak neutral current

Daniel Z. Freedman†
National Accelerator Laboratory, Batavia, Illinois 60510
and Institute for Theoretical Physics, State University of New York, Stony Brook, New York 11790
(Received 15 October 1973; revised manuscript received 19 November 1973)

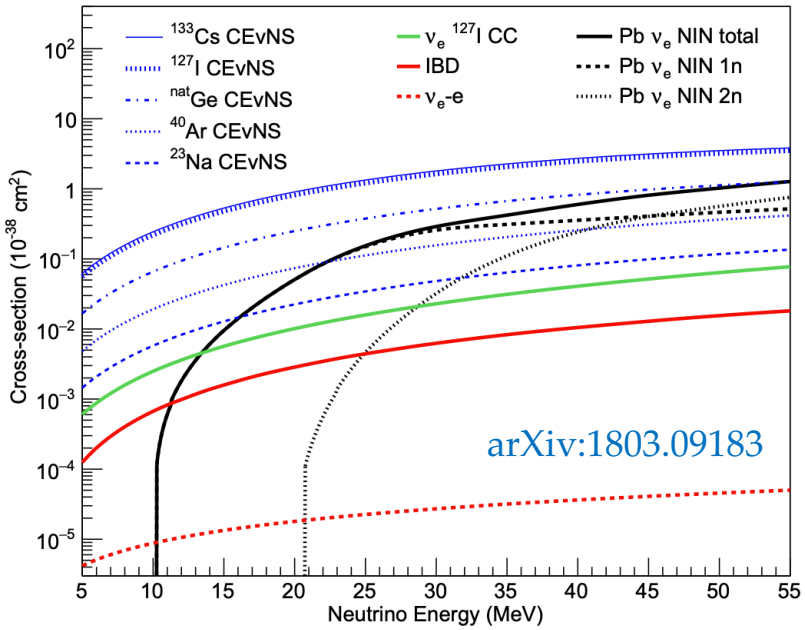

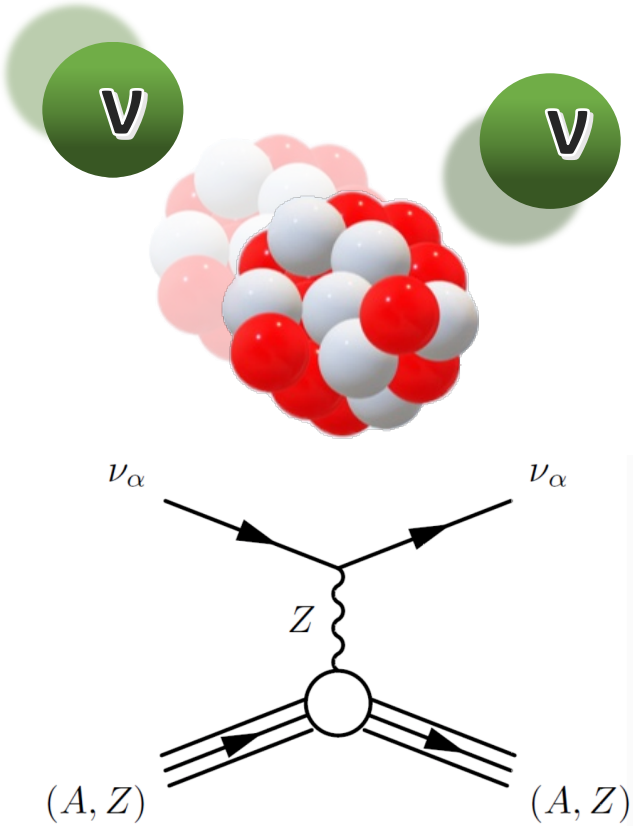

VERY CHALLENGING DETECTION!

Kinematic condition for CEvNS

$$|\vec{q}| \cdot R_N \ll 1$$

Small momentum transfer means small **recoil energy**:
MeV-neutrinos produce recoil energy around O(1-10) **keV.**

E = 30 MeV Cs: 14 keV Xe: 15 keV Ar: 48 keV

Standard Model cross section for CEvNS

The differential cross section as a function of the recoil energy for a spinless target is :

$$\frac{d\sigma_{\nu_\ell\text{-}\mathcal{N}}}{dT_{\rm nr}}(E,T_{\rm nr}) = \frac{G_{\rm F}^2 M}{\pi}\left(1-\frac{MT_{\rm nr}}{2E^2}\right)\left[g_V^p Z F_Z(|\vec{q}|^2) + g_V^n N F_N(|\vec{q}|^2)\right]^2$$

Tree Level

$$g_V^p = \frac{1}{2} - 2\sin^2\vartheta_W, \qquad g_V^n = -\frac{1}{2}$$

*Even if the target is not spin zero, the axial part remains negligible with respect to the vector part. The ratio of axial to vector contributions is expected to be of order of 1/A.

With radiative corrections

$$g_V^p(\nu_\ell) = \rho\left(\frac{1}{2} - 2\sin^2\vartheta_W\right) - \frac{\hat{\alpha}_Z}{4\pi\hat{s}_Z^2}\left(1 - 2\frac{\hat{\alpha}_s(m_W)}{\pi}\right) + \frac{\alpha}{6\pi}\left(3 - 2\ln\frac{m_\ell^2}{m_W^2}\right)$$

$$g_V^n = -\frac{\rho}{2} - \frac{\hat{\alpha}_Z}{8\pi\hat{s}_Z^2}\left(7 - 5\frac{\hat{\alpha}_s(m_W)}{\pi}\right)$$

J. Erler & S. Su - Prog.Part.Nucl.Phys. 71 (2013)
M. Cadeddu et al. - Phys.Rev.D 102 (2020) 1, 015030

Parameters included in the cross section

G_F	= Fermi constant	Z	= Number of protons	$\hat{\alpha}_s(m_W)$	= Strong coupling constant at W mass
M	= Mass of the target nucleus	N	= Number of neutrons	$\hat{\alpha}_Z$	= Fine structure constant at Z-mass
T_{nr}	= Recoil energy of the nucleus	F_Z	= Proton form factor	ρ	= Low-energy NC parameter
E	= Neutrino energy	F_N	= Neutron form factor	m_W	= Mass of W boson
g_V^p	= Vector coupling with protons	q	= Momentum transfer	m_ℓ	= Mass of the lepton
g_V^n	= Vector coupling with neutrons	ϑ_W	= Weinberg Angle	$\hat{s}_Z$	= $\sin^2\vartheta_W$ at the Z-boson mass

CEvNS detection by COHERENT Collaboration

Neutrino production at Spallation Neutron Source

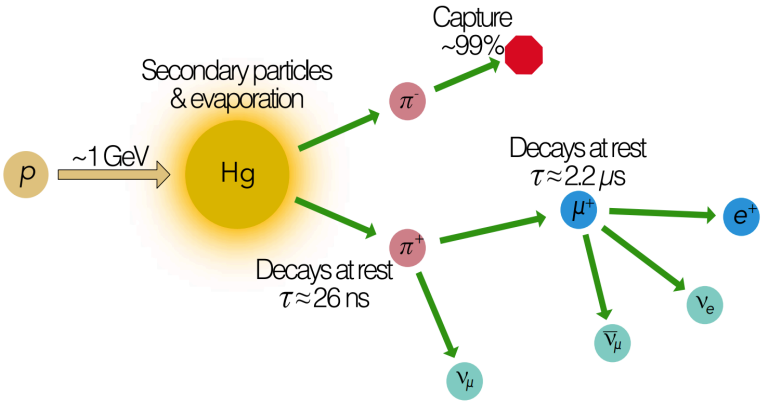

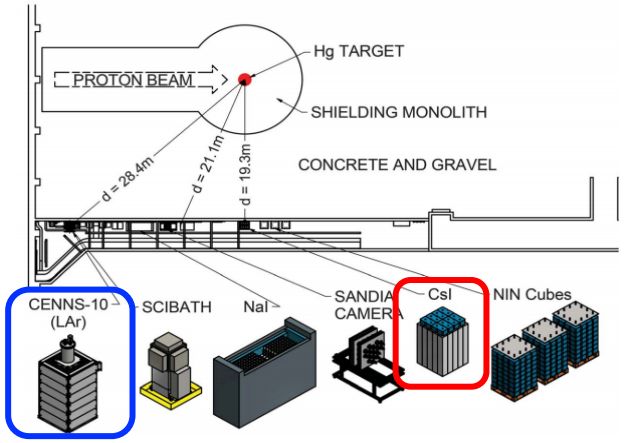

Cesium-Iodide

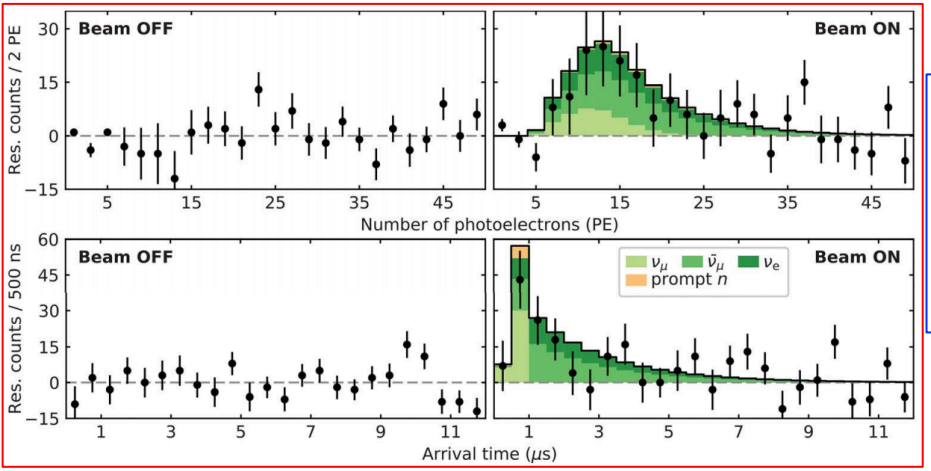

6.7σ C.L. 14.6 kg detector

Observation of Coherent Elastic Neutrino-Nucleus Scattering - COHERENT Collaboration (Akimov, D. et al.) Science 357 (2017) no.6356

Argon

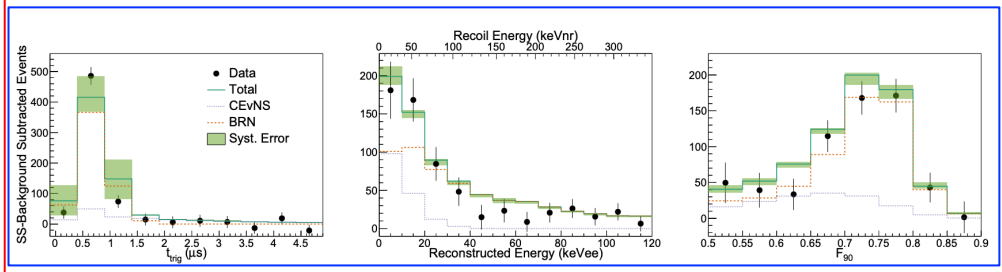

3.5σ C.L. 24 kg detector

First Detection of Coherent Elastic Neutrino-Nucleus Scattering on Argon - COHERENT Collaboration (Akimov, D. et al.) arXiv:2003.10630 [nucl-ex]

How to compare model with COHERENT data

The expected CEvNS signal is given by:

$$N_i^{\mathrm{CE}\nu\mathrm{NS}} = N(X) \int_{T_{\mathrm{nr}}^i}^{T_{\mathrm{nr}}^{i+1}} dT_{\mathrm{nr}} A(T_{\mathrm{nr}}) \int_{E_{\mathrm{min}}}^{E_{\mathrm{max}}} dE \sum_{\nu=\nu_e,\nu_\mu,\bar{\nu}_\mu} \frac{dN_\nu}{dE} \frac{d\sigma_{\nu-\mathcal{N}}}{dT_{\mathrm{nr}}}(E, T_{\mathrm{nr}})$$

- $N(X)$: Number of nuclei in the active volume of the detector
- $A(T_{nr})$: Acceptance of the detector
- dN_ν/dE : Neutrino fluxes at SNS
- $d\sigma/dT_{nr}$: CEvNS cross section

*The conversion between nuclear recoil and the measured observable includes the presence of **quenching factor,** a very challenging quantity to be measured, that for both CsI and Ar detectors is one of the parameter that affects the sensitivity of the experiment

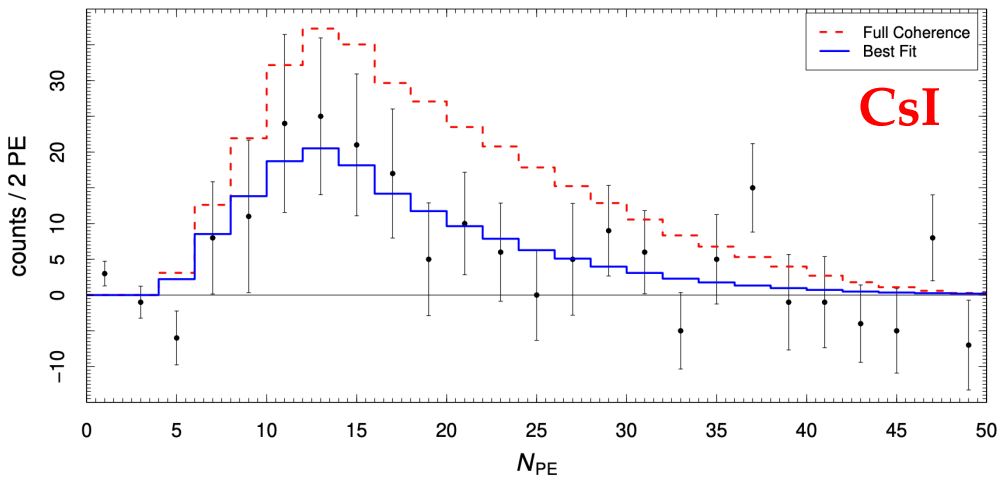

M. Cadeddu et al. - Phys.Rev.D 101 (2020) 3, 033004

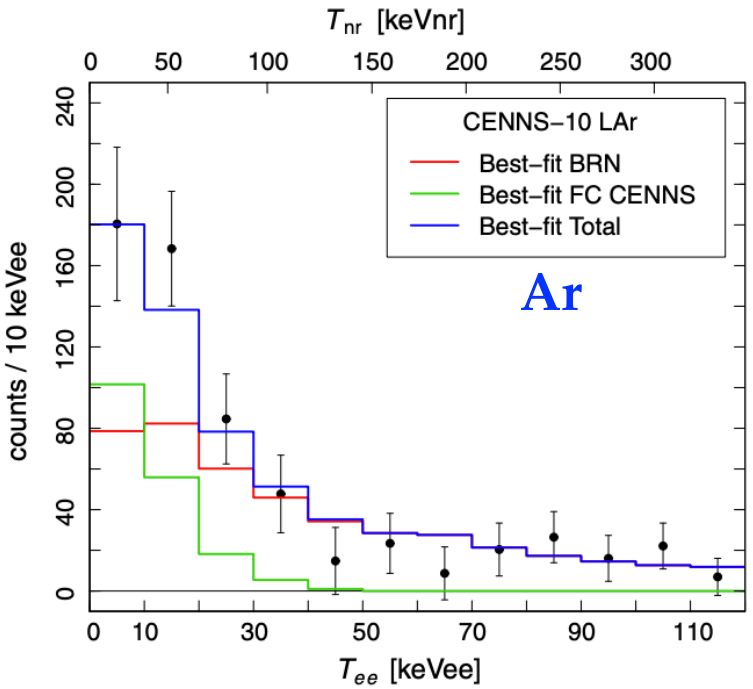

M. Cadeddu et al. - Phys.Rev.D 102 (2020) 1, 015030

Non Standard Interactions

The general vector neutral-current neutrino non standard interactions described by the effective four-fermion Lagrangian is:

$$\mathcal{L}_{\rm NSI}^{\rm NC} = -2\sqrt{2}G_{\rm F} \sum_{\alpha,\beta=e,\mu,\tau} (\overline{\nu_{\alpha L}}\gamma^{\rho}\nu_{\beta L}) \sum_{f=u,d} \varepsilon_{\alpha\beta}^{fV} (\bar{f}\gamma_{\rho}f)$$

SM electroweak vector contribution

$$Q_{\alpha}^2 = \left[g_V^p Z F_Z(|\vec{q}|^2) + g_V^n N F_N(|\vec{q}|^2)\right]^2$$

General NSI electroweak vector contribution

$$Q_{\alpha}^2 = \left[\left(g_V^p + 2\varepsilon_{\alpha\alpha}^{uV} + \varepsilon_{\alpha\alpha}^{dV}\right) Z F_Z(|\vec{q}|^2) + \left(g_V^n + \varepsilon_{\alpha\alpha}^{uV} + 2\varepsilon_{\alpha\alpha}^{dV}\right) N F_N(|\vec{q}|^2)\right]^2 + \sum_{\beta\neq\alpha} \left|\left(2\varepsilon_{\alpha\beta}^{uV} + \varepsilon_{\alpha\beta}^{dV}\right) Z F_Z(|\vec{q}|^2) + \left(\varepsilon_{\alpha\beta}^{uV} + 2\varepsilon_{\alpha\beta}^{dV}\right) N F_N(|\vec{q}|^2)\right|^2,$$

C. Giunti - Phys.Rev.D 101 (2020) 3, 035039

Assuming that neutrinos don't change flavor and only electron and muon neutrinos are involved in the process (as the case of COHERENT experiment):

$$\mathcal{L}_{\rm NSI}^{\rm NC} = -2\sqrt{2}G_F \sum_{\ell=e,\mu} (\overline{\nu_{\ell L}}\gamma^{\rho}\nu_{\ell L}) \sum_{f=u,d} \varepsilon_{\ell\ell}^{fV} (\bar{f}\gamma_{\rho}f)$$

No flavor changing NSI electroweak vector contribution

$$Q_{\ell}^2 = [(g_V^p(\nu_\ell) + 2\varepsilon_{\ell\ell}^{uV} + \varepsilon_{\ell\ell}^{dV}) Z F_Z(|\vec{q}|^2) + (g_V^n + \varepsilon_{\ell\ell}^{uV} + 2\varepsilon_{\ell\ell}^{dV}) N F_N(|\vec{q}|^2)]$$

*In principle we should also consider an axial contribution but in experiments looking for coherent scattering the axial contribution is negligible

Interactions mediated by non standard bosons

What if neutrino NSI are induced by a gauge Z'-boson with mass $M_{Z'}$ and coupling $g_{Z'}$ associated with a new U(1)' symmetry?

$$\varepsilon_{\ell\ell}^{fV} = \frac{g_{Z'}^2 Q'_\ell Q'_f}{\sqrt{2} G_F (|\vec{q}|^2 + M_{Z'}^2)}$$

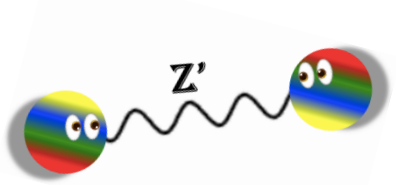

Depending on how the **new light vector mediator** couples to the SM, namely assuming a value for Q_ℓ and Q_f it is possible to explore several models, for instance the following three:

Universal model

J. Liao and D. Marfatia- *Phys.Lett.B* 775 (2017)

$$\left(\frac{d\sigma}{dT_{\rm nr}}\right)^{\nu_\ell\text{-}\mathcal{N}}_{\rm univ}(E, T_{\rm nr}) = \frac{G_F^2 M}{\pi}\left(1 - \frac{M T_{\rm nr}}{2E^2}\right) \cdot \left[Q_{\ell,\rm SM} + \frac{3(g_{Z'})^2}{\sqrt{2}G_F}\frac{Z F_Z(|\vec{q}|^2) + N F_N(|\vec{q}|^2)}{|\vec{q}|^2 + M_{Z'}^2}\right]^2$$

B-L model

T. Han, J. Liao, H. Liu and D. Marfatia - JHEP 11 (2019) 028
J. Billard, J. Johnston and B.J. Kavanagh - JCAP 11 (2018) 016

$$\left(\frac{d\sigma}{dT_{\rm nr}}\right)^{\nu_\ell\text{-}\mathcal{N}}_{\rm B-L}(E, T_{\rm nr}) = \frac{G_F^2 M}{\pi}\left(1 - \frac{M T_{\rm nr}}{2E^2}\right) \cdot \left[Q_{\ell,\rm SM} - \frac{(g_{Z'})^2}{\sqrt{2}G_F}\frac{Z F_Z(|\vec{q}|^2) + N F_N(|\vec{q}|^2)}{|\vec{q}|^2 + M_{Z'}^2}\right]^2$$

L_μ-L_τ model

W. Altmannshofer et al. - Phys. Rev. D 100 (2019) 115029

$$\left(\frac{d\sigma}{dT_{\rm nr}}\right)^{\nu_\ell\text{-}\mathcal{N}}_{L_\mu - L_\tau}(E, T_{\rm nr}) = \frac{G_F^2 M}{\pi}\left(1 - \frac{M T_{\rm nr}}{2E^2}\right) \cdot$$
$$\left\{\left[g_V^p(\nu_\ell) - \frac{\alpha_{\rm EM}\,(g_{Z'})^2}{3\sqrt{2}\pi G_F}\log\left(\frac{m_\tau^2}{m_\mu^2}\right)\frac{1}{|\vec{q}|^2 + M_{Z'}^2}\right] Z F_Z(|\vec{q}|^2) + g_V^n N F_N(|\vec{q}|^2)\right\}^2$$

Interactions mediated by non standard bosons

How does the COHERENT theoretical rate of events change with Z′ contributions?

Universal model

Low energy:
Enhancement of the rate

High energy:
Drop of the rate due the cancellation of the cross section

B-L model

L_μ-L_τ model

Overall enhancement of the event rate

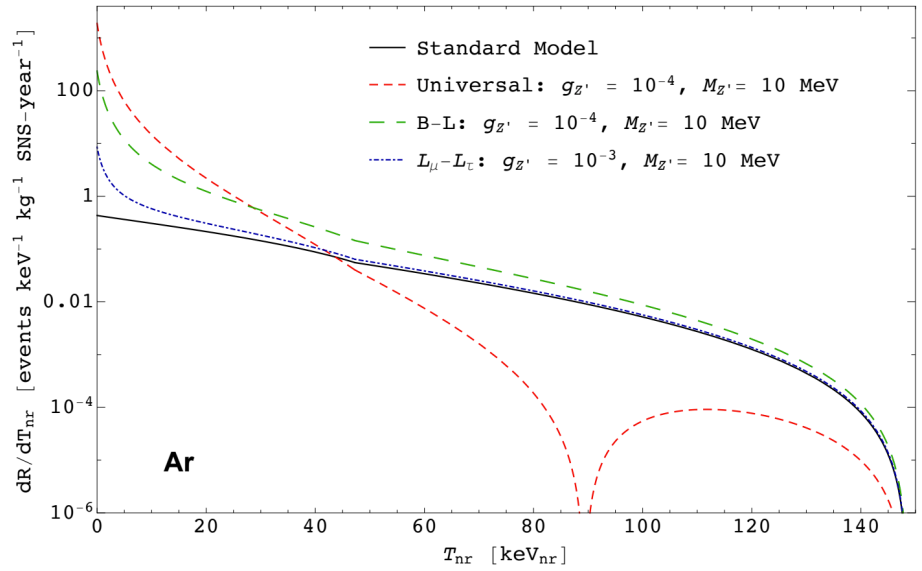

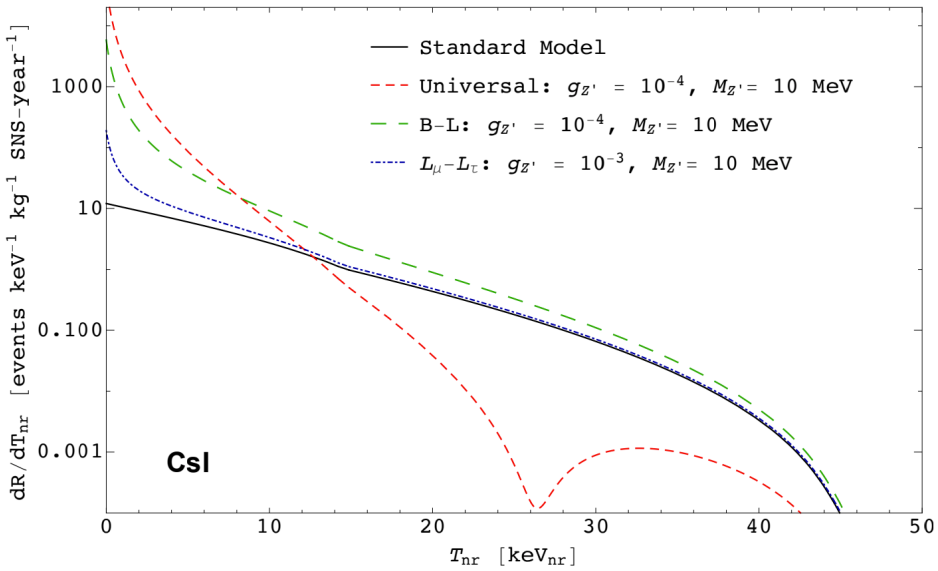

Constraints on the 3 models using COHERENT data

Universal model

- Improved limits for $M_{Z'} > 4$ MeV
- Degeneracy line related to the cancellation in the event rate

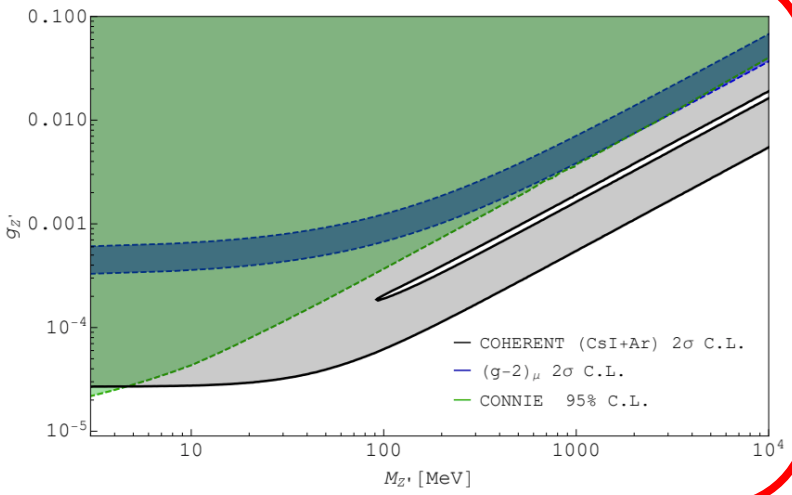

B-L

Improved limits for 20 MeV < $M_{Z'}$ < 200 MeV

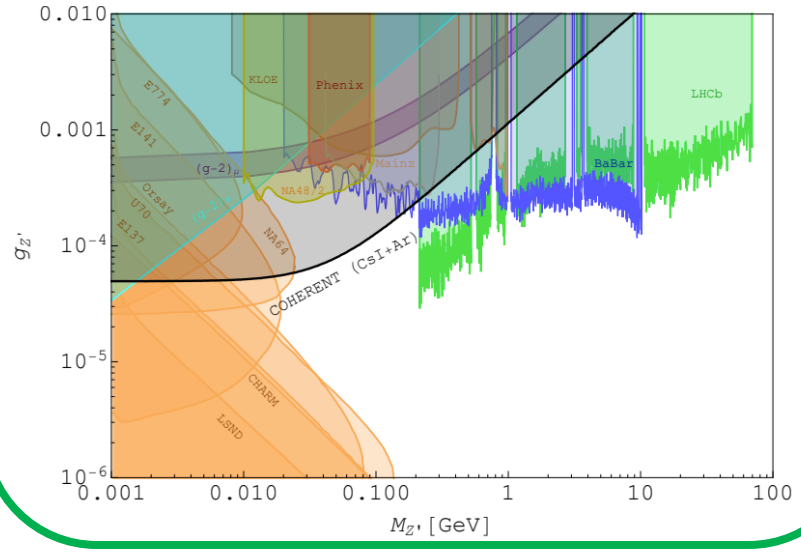

L_μ-L_τ

- Confirmation of already set limits.
- Promising opportunity to improve limits with next COHERENT phase

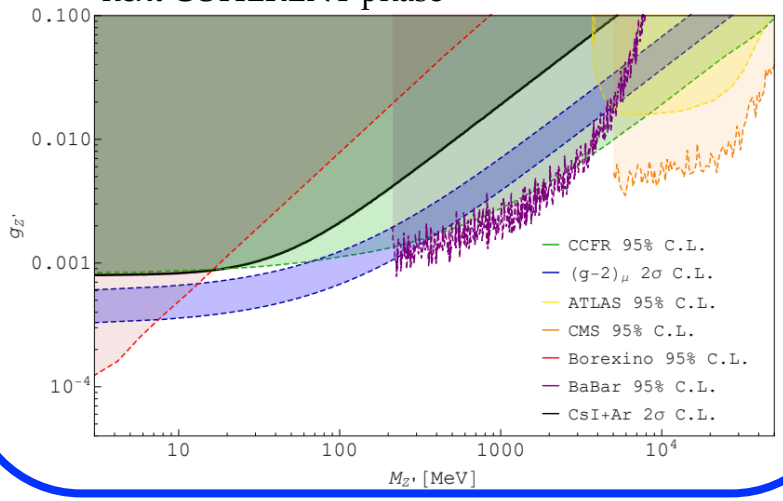

Thanks for the attention


YOU MISSED SOMETHING
SCROLL BACK UP

CEvNS cross section and measurable parameters

The differential cross section as a function of the recoil energy for a spinless target is :

$$\frac{d\sigma_{\nu_\ell\text{-}\mathcal{N}}}{dT_{\rm nr}}(E,T_{\rm nr}) = \frac{G_{\rm F}^2 M}{\pi}\left(1-\frac{MT_{\rm nr}}{2E^2}\right)\left[g_V^p Z F_Z(|\vec{q}|^2) + g_V^n N F_N(|\vec{q}|^2)\right]^2$$

Electroweak vector coupling

$$C_V = g_V^p Z F_Z(|\vec{q}|^2) + g_V^n N F_N(|\vec{q}|^2)$$
$$= \frac{1}{2}[(1-4\sin^2\vartheta_W) Z F_Z(|\vec{q}|^2) - N F_N(|\vec{q}|^2)]$$

Weak mixing angle

Neutron Form Factor

$$F(q)^{\rm Helm} = 3\frac{j_1(qR_0)}{qR_0}e^{-\frac{(qs)^2}{2}}$$

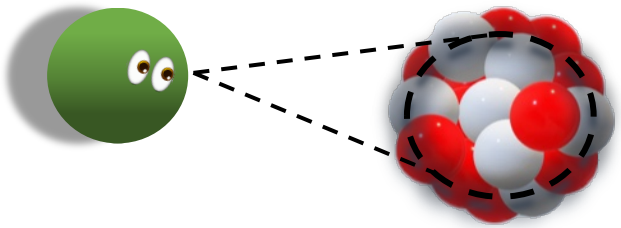

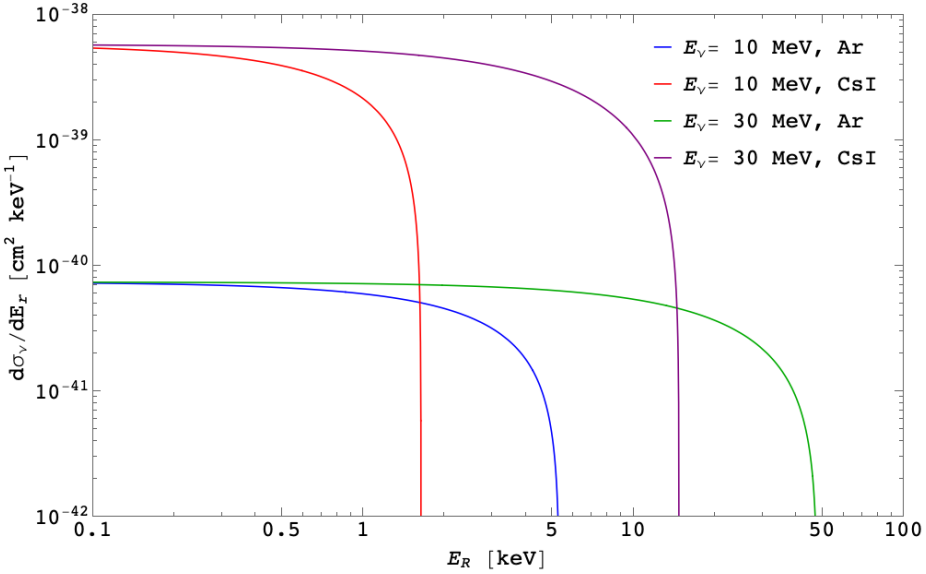

Measurements:

- ϑ_W gives information about weak interactions
- R_0 gives information about how neutrons are distributed in the nucleus

CEvNS detection by COHERENT Collaboration

Neutrino production at Spallation Neutron Source

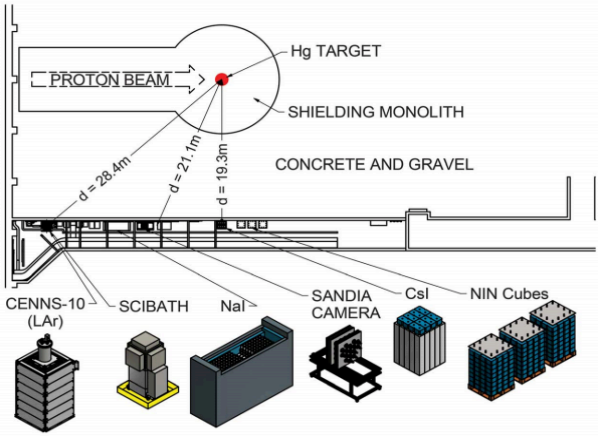

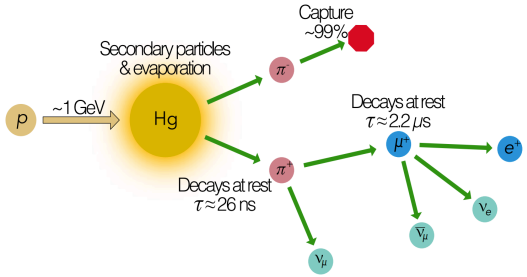

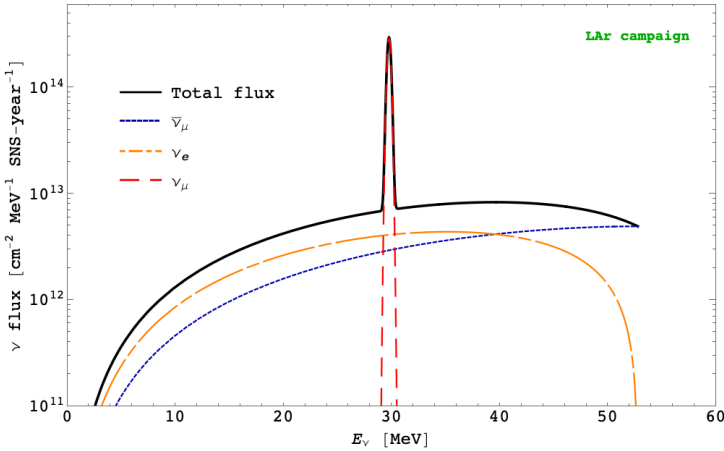

First detection ever

Oct 1973: **Prediction**
Aug 2017: **Discovery**

Observation of the process at **6.7σ** CL using 14.6 kg CsI low-background scintillator as a target

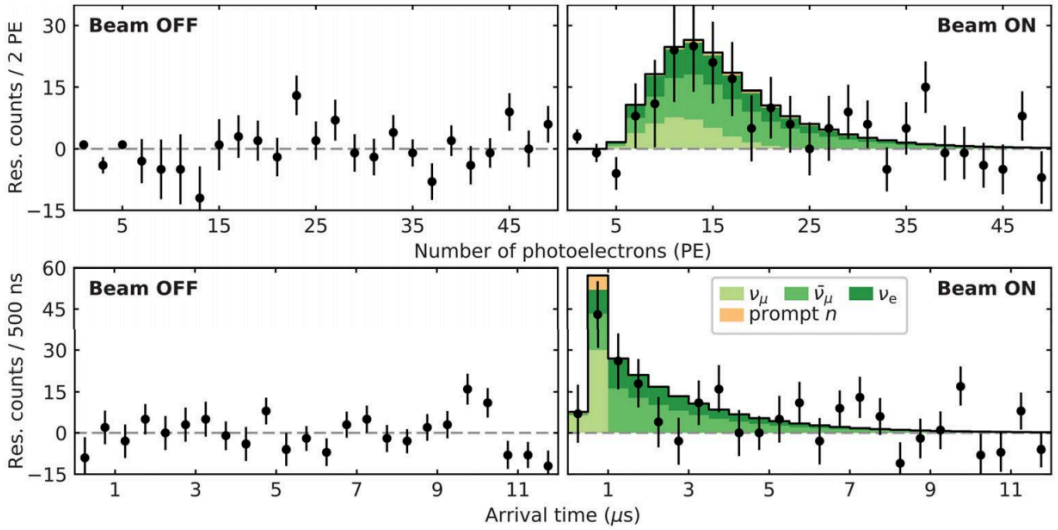

First detection of CEvNS in liquid argon detector

In 2020 also COHERENT LAr detector has seen CEvNS!

SIGNAL: CEvNS interaction with Ar nuclei ⟹ Nuclear recoils

BACKGROUND: Neutrons interaction with Ar nuclei ⟹ Nuclear recoils

Gamma and beta interaction with Ar ⟹ Electron recoils

With LAr detectors it is possible to exploit a very powerful tool (Pulse Shape Discrimination) that allows to reject most of the background produced by electron recoils

DATA RELEASE

Time of the event with respect to the start time of the beam

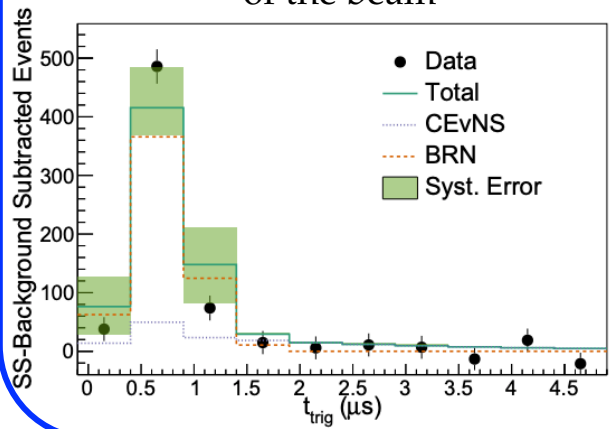

Recoil energy of the event

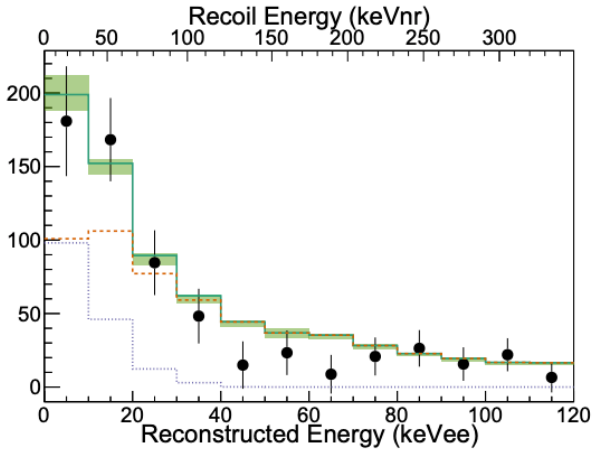

PSD value of the event

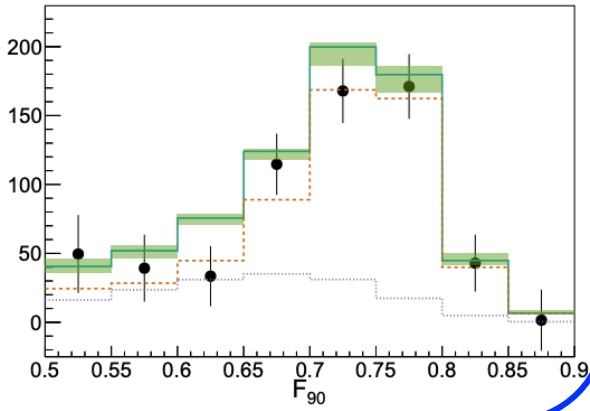

Evidence of the process at **3.5σ** CL using 24 kg of atmospheric ^{40}Ar.

Measurements exploiting COHERENT data

The expected CEvNS signal is given by:

$$N_i^{\mathrm{CE}\nu\mathrm{NS}} = N(\mathrm{Ar}) \int_{T_{\mathrm{nr}}^i}^{T_{\mathrm{nr}}^{i+1}} dT_{\mathrm{nr}}\, A(T_{\mathrm{nr}}) \int_{E_{\mathrm{min}}}^{E_{\mathrm{max}}} dE \sum_{\nu=\nu_e,\nu_\mu,\overline{\nu}_\mu} \frac{dN_\nu}{dE} \frac{d\sigma_{\nu\text{-}\mathcal{N}}}{dT_{\mathrm{nr}}}(E, T_{\mathrm{nr}})$$

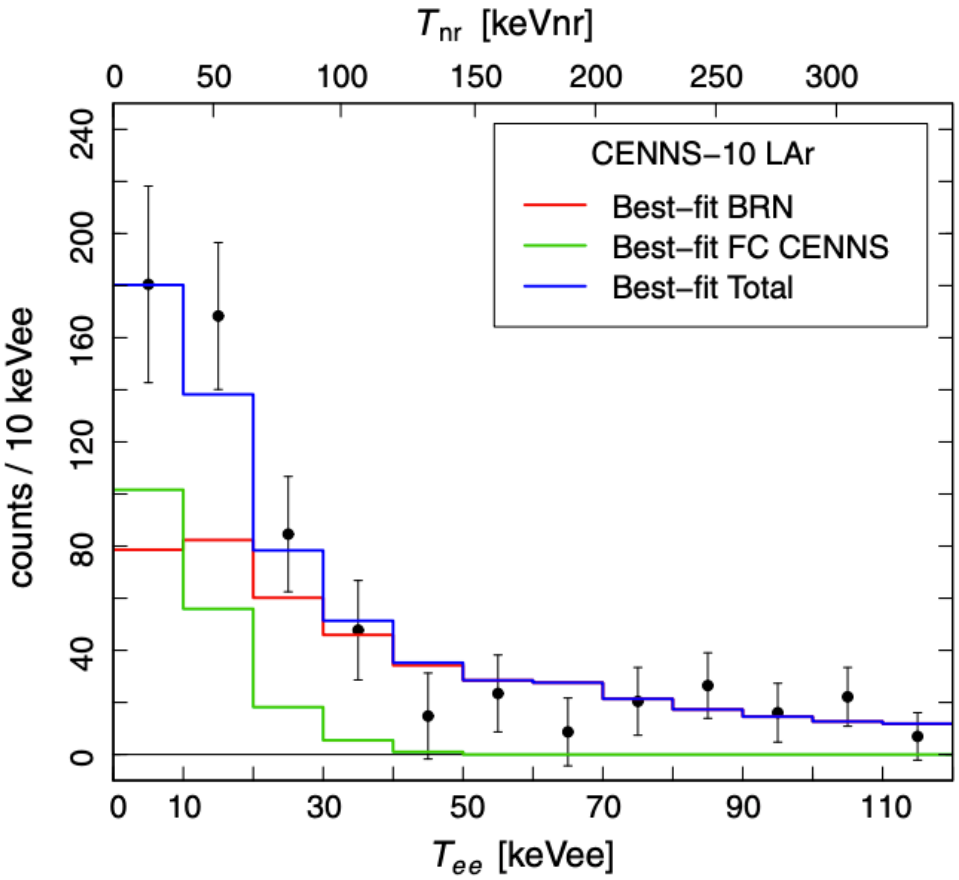

$N(Ar)$: Number of nuclei in the active volume of the detector

$A(T_{nr})$: Acceptance of the detector

dN_ν/dE : Neutrino fluxes at SNS

$d\sigma/dT_{nr}$: CEvNS cross section

Measurements exploiting COHERENT data

We performed a χ^2 fit of the data measuring:

Neutron distribution radius

The neutron form factor embeds the neutron distribution radius

Nuclear models prediction: $3.45\ \text{fm} < R_n(^{40}\text{Ar}) < 4\ \text{fm}$

Our result

$$R_n(^{40}\text{Ar}) < 4.2(1\sigma), 6.2(2\sigma), 10.8(3\sigma)\ \text{fm}$$

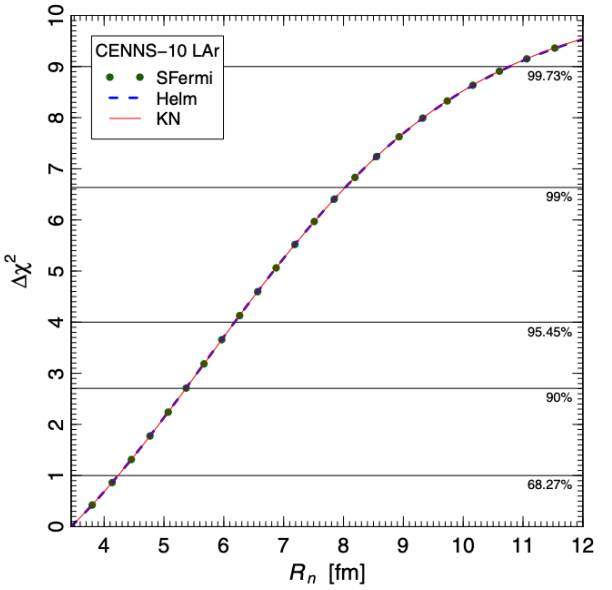

Weak Mixing Angle

Theoretical prediction: $\sin^2\vartheta_W = 0.23857 \pm 0.00005$

Our result

$$\sin^2\vartheta_W(\text{Ar}) = 0.31 \pm 0.06\,(1\sigma), ^{+0.11}_{-0.13}\,(2\sigma), ^{+0.18}_{-0.23}\,(3\sigma)$$

$$\sin^2\vartheta_W(\text{CsI}) = 0.24 \pm 0.04\,(1\sigma), \pm 0.09\,(2\sigma), ^{+0.13}_{-0.14}\,(3\sigma)$$

$$\sin^2\vartheta_W(\text{CsI} + \text{Ar}) = 0.26^{+0.04}_{-0.03}\,(1\sigma), \pm 0.07\,(2\sigma), \pm 0.11\,(3\sigma)$$

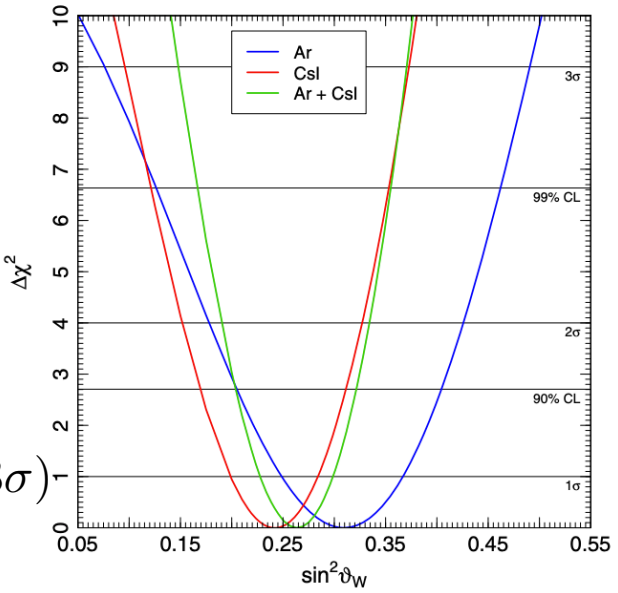

Measuraments exploiting COHERENT data

We performed a χ^2 fit of the data measuring:

Neutrino charge radii

The cross section is modified by the presence of neutrino charge radii

$$\frac{d\sigma_{\nu_\ell\text{-}\mathcal{N}}}{dT_{\rm nr}}(E,T_{\rm nr}) = \frac{G_{\rm F}^2 M}{\pi}\left(1-\frac{MT_{\rm nr}}{2E^2}\right)\left\{\left[\left(\tilde{g}_V^p-\tilde{Q}_{\ell\ell}\right)ZF_Z(|\vec{q}|^2)+g_V^n NF_N(|\vec{q}|^2)\right]^2+Z^2F_Z^2(|\vec{q}|^2)\sum_{\ell'\neq\ell}|\tilde{Q}_{\ell'\ell}|^2\right\}$$

Charge radius contribution: $\tilde{Q}_{\ell\ell'} = \dfrac{\sqrt{2}\pi\alpha}{3G_{\rm F}}\langle r^2_{\nu_{\ell\ell'}}\rangle$

Theoretical prediction:

$$\langle r^2_{\nu_\mu}\rangle_{\rm SM} = -0.48\times10^{-32}\,{\rm cm}^2$$
$$\langle r^2_{\nu_e}\rangle_{\rm SM} = -0.83\times10^{-32}\,{\rm cm}^2$$

Our result

	Fixed R_n			Free R_n		
	1σ	2σ	3σ	1σ	2σ	3σ
CsI						
$\langle r^2_{\nu_{ee}}\rangle$	$-55\div-2$	$-67\div11$	$-76\div20$	$-54\div1$	$-66\div14$	$-76\div24$
$\langle r^2_{\nu_{\mu\mu}}\rangle$	$-64\div8$	$-68\div12$	$-73\div17$	$-64\div10$	$-68\div15$	$-72\div20$
$\langle r^2_{\nu_{e\mu}}\rangle$	<26	<32	<37	<26	<32	<36
$\langle r^2_{\nu_{e\tau}}\rangle$	<27	<39	<48	<27	<39	<48
$\langle r^2_{\nu_{\mu\tau}}\rangle$	<36	<40	<45	<36	<40	<45
Ar						
$\langle r^2_{\nu_{ee}}\rangle$	$-89\div39$	$-98\div48$	$-108\div58$	$-89\div38$	$-97\div47$	$-107\div57$
$\langle r^2_{\nu_{\mu\mu}}\rangle$	$-63\div12$	$-73\div22$	$-80\div30$	$-63\div9$	$-72\div22$	$-80\div29$
$\langle r^2_{\nu_{e\mu}}\rangle$	<34	<40	<46	<33	<40	<46
$\langle r^2_{\nu_{e\tau}}\rangle$	<64	<73	<83	<63	<72	<82
$\langle r^2_{\nu_{\mu\tau}}\rangle$	<37	<48	<55	<36	<47	<54
CsI + Ar						
$\langle r^2_{\nu_{ee}}\rangle$	$-56\div-2$	$-68\div11$	$-78\div22$	$-55\div-4$	$-67\div14$	$-77\div25$
$\langle r^2_{\nu_{\mu\mu}}\rangle$	$-64\div6$	$-68\div12$	$-71\div17$	$-64\div9$	$-67\div15$	$-71\div19$
$\langle r^2_{\nu_{e\mu}}\rangle$	<27	<33	<36	<25	<32	<36
$\langle r^2_{\nu_{e\tau}}\rangle$	<27	<40	<50	<26	<40	<50
$\langle r^2_{\nu_{\mu\tau}}\rangle$	<36	<40	<44	<36	<40	<44

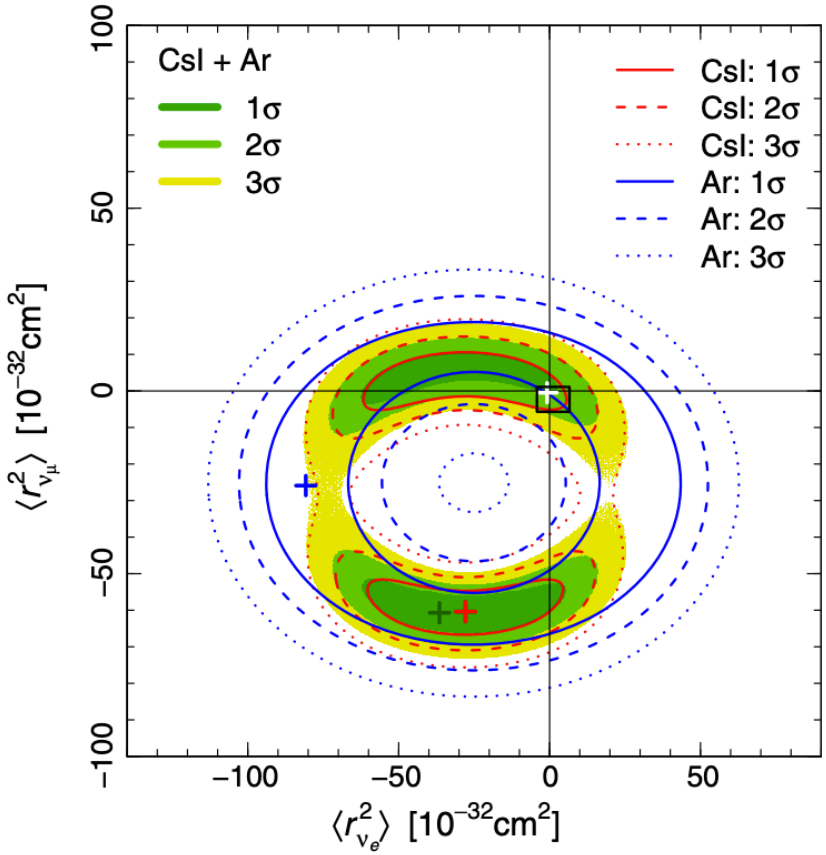

Measurements exploiting COHERENT data

We performed a χ^2 fit of the data measuring:

Neutrino electric charge

The cross section is modified by the presence of neutrino electric charge

$$\frac{d\sigma_{\nu_\ell\text{-}\mathcal{N}}}{dT_{\rm nr}}(E,T_{\rm nr}) = \frac{G_{\rm F}^2 M}{\pi}\left(1-\frac{MT_{\rm nr}}{2E^2}\right)\left\{\left[\left(g_V^p - Q_{\ell\ell}\right)ZF_Z(|\vec{q}|^2) + g_V^n N F_N(|\vec{q}|^2)\right]^2 + Z^2F_Z^2(|\vec{q}|^2)\sum_{\ell'\neq\ell}|Q_{\ell'\ell}|^2\right\}$$

Electric charge contribution: $Q_{\ell\ell'} = \dfrac{2\sqrt{2}\pi\alpha}{G_{\rm F}q^2}\, q_{\nu_{\ell\ell'}}$

Theoretical prediction:

$$q_{\nu_{\ell\ell'}}^{\rm SM} = 0$$

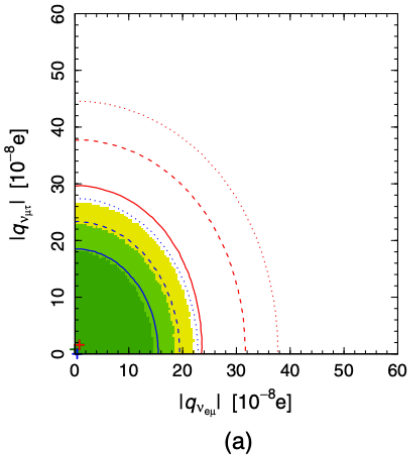

Our result

	Fixed R_n			Free R_n		
	1σ	2σ	3σ	1σ	2σ	3σ
			CsI			
$q_{\nu_{ee}}$	$0 \div 37$	$-13 \div 57$	$-24 \div 71$	$0 \div 39$	$-15 \div 57$	$-27 \div 71$
$q_{\nu_{\mu\mu}}$	$-8 \div 8$	$-13 \div 27$	$-19 \div 47$	$-8 \div 9$	$-14 \div 28$	$-20 \div 47$
$\lvert q_{\nu_{e\mu}}\rvert$	< 17	< 28	< 35	< 18	< 28	< 35
$\lvert q_{\nu_{e\tau}}\rvert$	< 23	< 38	< 51	< 23	< 38	< 51
$\lvert q_{\nu_{\mu\tau}}\rvert$	< 23	< 34	< 41	< 24	< 34	< 41
			Ar			
$q_{\nu_{ee}}$	$-17 \div 18$	$-23 \div 38$	$-28 \div 47$	$-16 \div 18$	$-23 \div 38$	$-28 \div 47$
$q_{\nu_{\mu\mu}}$	$-8 \div 14$	$-11 \div 28$	$-15 \div 35$	$-7 \div 14$	$-11 \div 28$	$-15 \div 35$
$\lvert q_{\nu_{e\mu}}\rvert$	< 12	< 18	< 21	< 12	< 17	< 21
$\lvert q_{\nu_{e\tau}}\rvert$	< 22	< 32	< 38	< 21	< 32	< 38
$\lvert q_{\nu_{\mu\tau}}\rvert$	< 14	< 21	< 25	< 14	< 21	< 25
			CsI + Ar			
$q_{\nu_{ee}}$	$-4 \div 24$	$-14 \div 34$	$-20 \div 42$	$-5 \div 23$	$-14 \div 34$	$-20 \div 41$
$q_{\nu_{\mu\mu}}$	$-7 \div 4$	$-10 \div 12$	$-12 \div 20$	$-7 \div 3$	$-10 \div 12$	$-13 \div 20$
$\lvert q_{\nu_{e\mu}}\rvert$	< 11	< 17	< 20	< 11	< 16	< 20
$\lvert q_{\nu_{e\tau}}\rvert$	< 18	< 27	< 34	< 17	< 27	< 33
$\lvert q_{\nu_{\mu\tau}}\rvert$	< 14	< 20	< 25	< 14	< 20	< 24

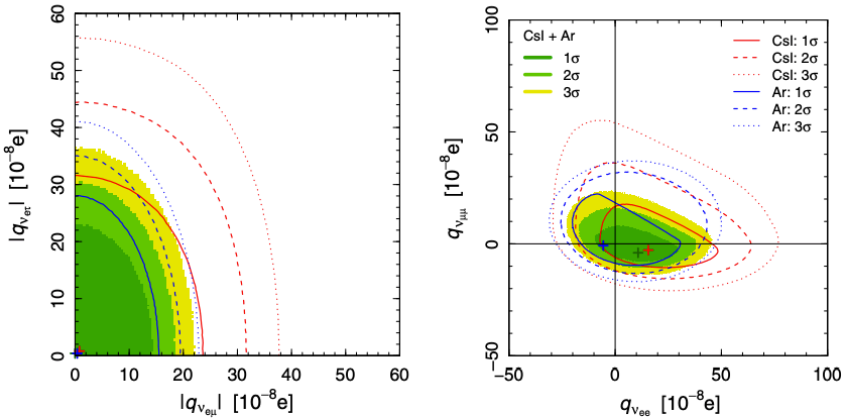

Measurements exploiting COHERENT data

We performed a χ^2 fit of the data measuring:

Neutrino magnetic moment

The presence of the magnetic moment adds a contribution to the cross section

$$\frac{d\sigma_{\nu_\ell\text{-}\mathcal{N}}}{dT_{\rm nr}}(E,T_{\rm nr}) = \frac{d\sigma^{\rm SM}_{\nu_\ell\text{-}\mathcal{N}}}{dT_{\rm nr}}(E,T_{\rm nr}) + \frac{d\sigma^{\rm mag}_{\nu_\ell\text{-}\mathcal{N}}}{dT_{\rm nr}}(E,T_{\rm nr})$$

Neutrino magnetic moment cross section:

$$\frac{d\sigma^{\rm mag}_{\nu_\ell\text{-}\mathcal{N}}}{dT_{\rm nr}}(E,T_{\rm nr}) = \frac{\pi\alpha^2}{m_e^2}\left(\frac{1}{T_{\rm nr}} - \frac{1}{E}\right) Z^2 F_Z^2(|\vec{q}|^2) \left|\frac{\mu_{\nu_\ell}}{\mu_{\rm B}}\right|^2$$

Theoretical prediction:

$$\mu_\nu = \frac{3\,e\,G_F}{8\sqrt{2}\,\pi^2} m_\nu \simeq 3.2\times 10^{-19}\left(\frac{m_\nu}{\rm eV}\right)\mu_B$$

Our result

	Fixed R_n			Free R_n		
	1σ	2σ	3σ	1σ	2σ	3σ
			CsI			
$\lvert\mu_{\nu_e}\rvert$	< 24	< 42	< 58	< 33	< 50	< 65
$\lvert\mu_{\nu_\mu}\rvert$	< 26	< 34	< 42	$3 \div 31$	< 39	< 46
			Ar			
$\lvert\mu_{\nu_e}\rvert$	< 55	< 70	< 85	< 55	< 70	< 85
$\lvert\mu_{\nu_\mu}\rvert$	< 39	< 50	< 60	< 39	< 50	< 60
			CsI + Ar			
$\lvert\mu_{\nu_e}\rvert$	< 27	< 44	< 56	< 33	< 48	< 60
$\lvert\mu_{\nu_\mu}\rvert$	$5 \div 27$	< 34	< 41	$12 \div 31$	< 37	< 43

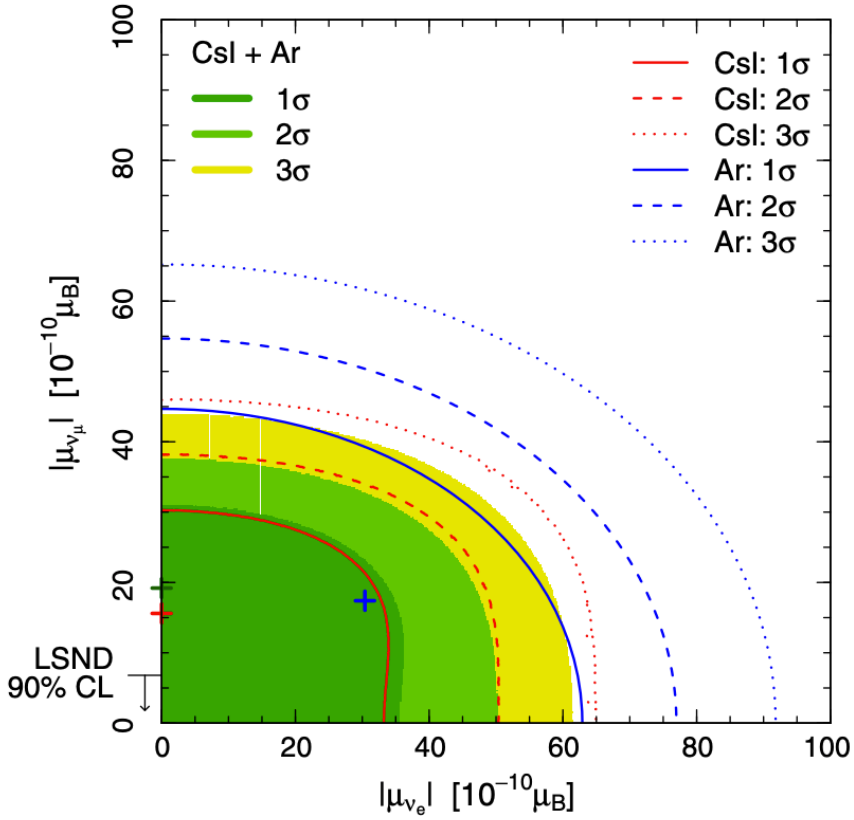

Neutron distribution radius

$$F(q)^{\text{Helm}} = 3\frac{j_1(qR_0)}{qR_0}e^{-\frac{(qs)^2}{2}}$$

Where j_1 is the Bessel function of first type, R_0 is called diffraction radius, very related with the nucleus rms radius, and s = 0.9 fm is the so-called surface thickness

TABLE I. Values of the ^{40}Ar point-proton radius R_p^{point} and point-neutron radius R_n^{point} obtained with the Sky3D [38] and DIRHB [39] codes with different nuclear interactions.

Interaction	R_p^{point}	R_n^{point}
Sky3D		
SkI3 [40]	3.33	3.43
SkI4 [40]	3.31	3.41
Sly4 [41]	3.38	3.46
Sly5 [41]	3.37	3.45
Sly6 [41]	3.36	3.44
Sly4d [42]	3.35	3.44
SV-bas [43]	3.33	3.42
UNEDF0 [44]	3.37	3.47
UNEDF1 [45]	3.33	3.43
SkM* [46]	3.37	3.45
SkP [47]	3.40	3.48
DIRHB		
DD-ME2 [48]	3.30	3.39
DD-PC1 [49]	3.30	3.39

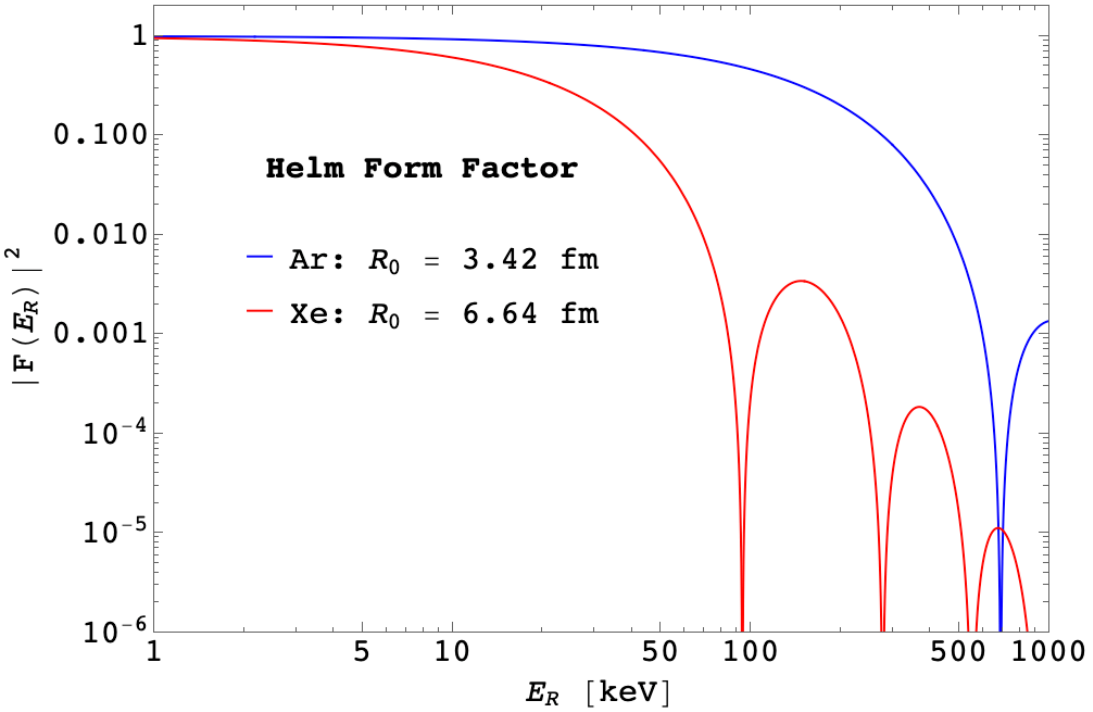

Naively, the form factor takes into account the size of the portion that neutrinos can see

$$R^2 = \frac{3}{5}R_0^2 + 3s^2$$

$$R_n^2 = (R_n^{\text{point}})^2 + \langle r_n^2 \rangle$$

$$R_n \simeq R_p + 0.1 \text{ fm}.$$

Neutrino fluxes at SNS

$$\frac{dN_{\nu_\mu}}{dE} = \eta\delta\left(E - \frac{m_\pi^2 - m_\mu^2}{2m_\pi}\right),$$

$$\frac{dN_{\nu_{\bar{\mu}}}}{dE} = \eta\frac{64E^2}{m_\mu^3}\left(\frac{3}{4} - \frac{E}{m_\mu}\right),$$

$$\frac{dN_{\nu_e}}{dE} = \eta\frac{192E^2}{m_\mu^3}\left(\frac{1}{2} - \frac{E}{m_\mu}\right),$$

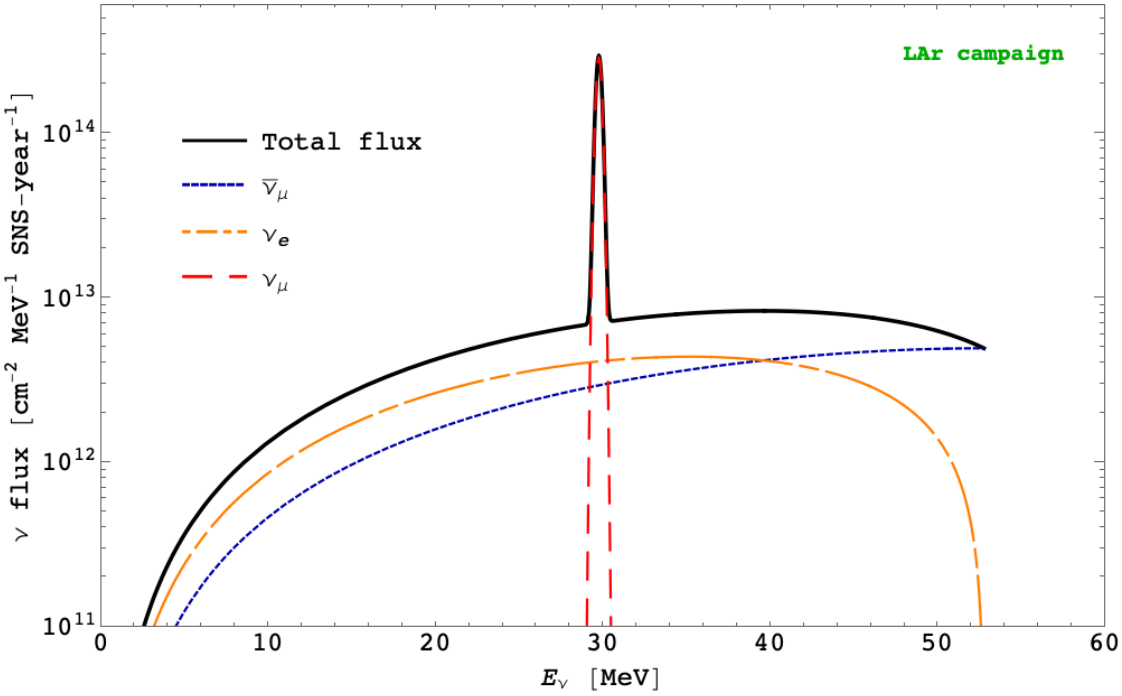

$$\eta = rN_{\mathrm{POT}}/4\pi L^2$$

$$r = (9 \pm 0.9) \times 10^{-2}$$

$L_{Ar} = 27.5\ m$ $\quad N_{POT,Ar} = 13.7{\times}10^{22}$

$L_{CsI} = 19.3\ m$ $\quad N_{POT,CsI} = 17.6{\times}10^{22}$

Spallation Neutron Source, ORNL

χ^2 definition and fit

$$\chi^2_S = \sum_{i=1}^{12} \left(\frac{N_i^{\rm exp} - \eta_{\rm CE\nu NS} N_i^{\rm CE\nu NS} - \eta_{\rm PBRN} B_i^{\rm PBRN} - \eta_{\rm LBRN} B_i^{\rm LBRN}}{\sigma_i} \right)^2 + \left(\frac{\eta_{\rm CE\nu NS} - 1}{\sigma_{\rm CE\nu NS}} \right)^2 + \left(\frac{\eta_{\rm PBRN} - 1}{\sigma_{\rm PBRN}} \right)^2 + \left(\frac{\eta_{\rm LBRN} - 1}{\sigma_{\rm LBRN}} \right)^2$$

$$\sigma_i^2 = (\sigma_i^{\rm exp})^2 + [\sigma_{\rm BRNES}(B_i^{\rm PBRN} + B_i^{\rm LBRN})]^2,$$

$$\sigma_{\rm BRNES} = \sqrt{\frac{0.058^2}{12}} = 1.7\%,$$

$$\sigma_{\rm CE\nu NS} = 13.4\% \text{ for fixed } R_n, \text{ or } 13.2\% \text{ for free } R_n,$$

$$\sigma_{\rm PBRN} = 32\%,$$

$$\sigma_{\rm LBRN} = 100\%.$$

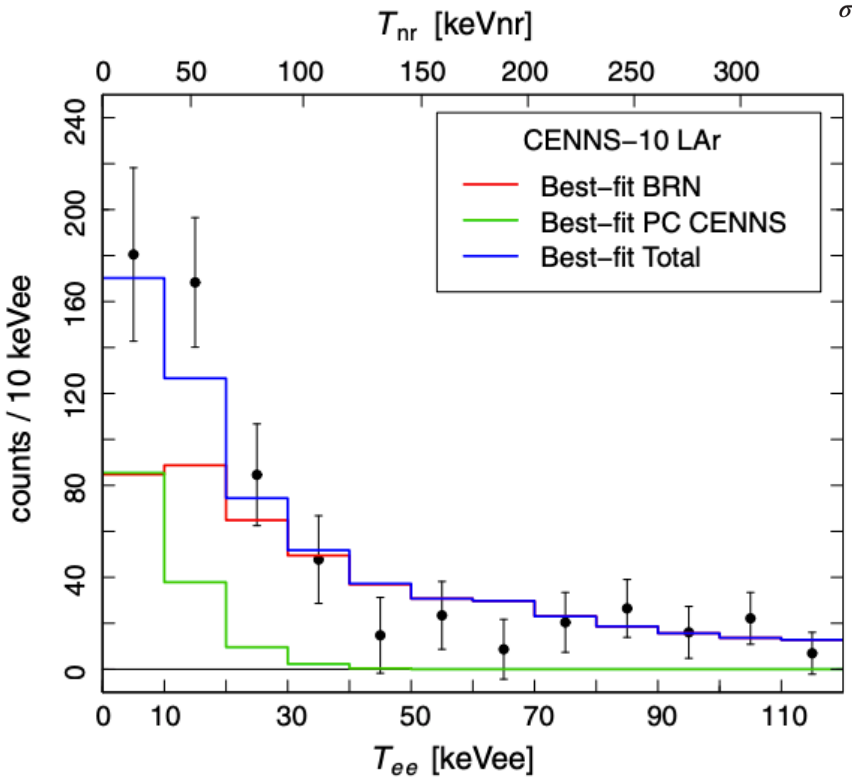

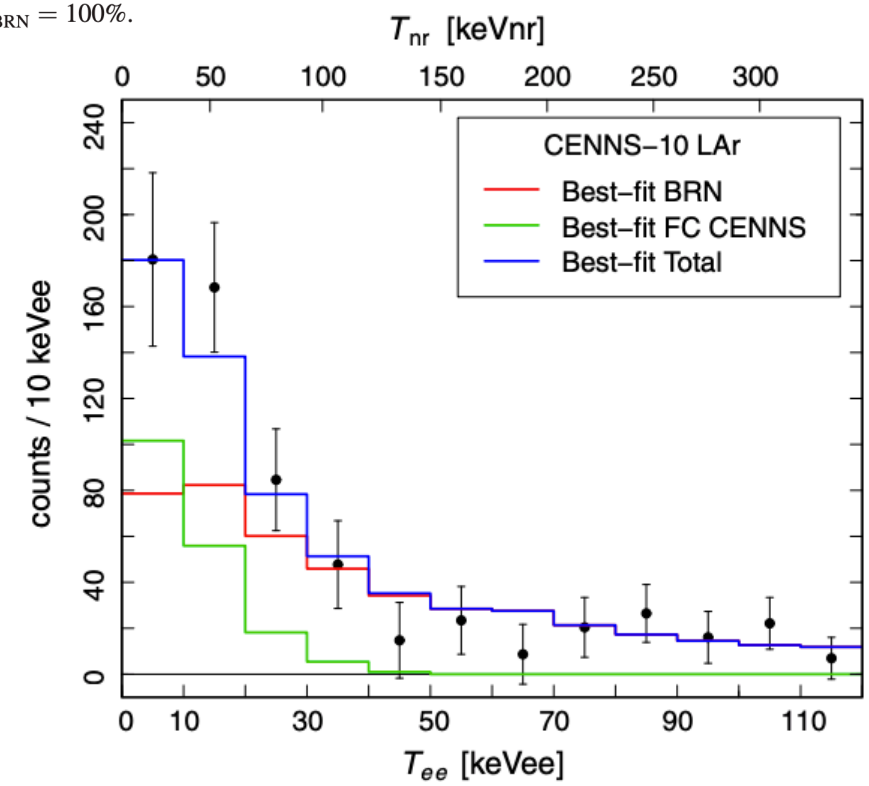

Quenching Factor

$$T_{ee} = f_Q(T_{\mathrm{nr}})T_{\mathrm{nr}}$$

Gives information about the number of photoelectrons released and the nuclear recoil energy

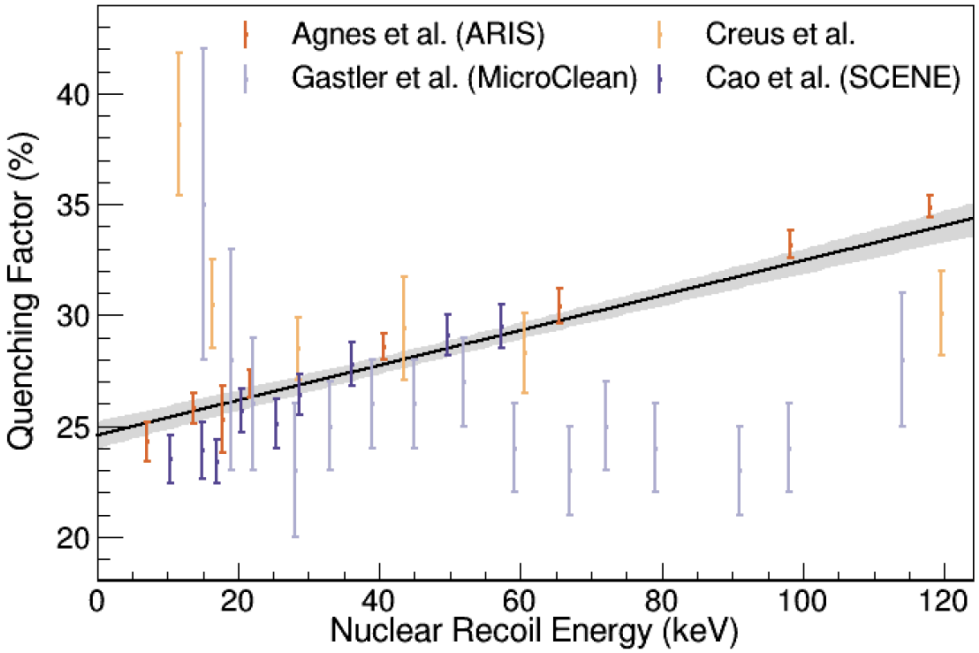

$$f_Q(T_{\mathrm{nr}}) = (0.246 \pm 0.006\,\mathrm{keV_{nr}}) + ((7.8 \pm 0.9) \times 10^{-4})T_{\mathrm{nr}}$$

Here, f_Q is the quenching factor, which is the ratio between the scintillation light emitted in nuclear and electron recoils and determines the relation between the number of detected photoelectrons and the nuclear recoil kinetic energy.

Neutrino Magnetic Moment

The neutrino magnetic moment arises at the one-loop level, as does the weak contribution to the anomalous magnetic moment of a charged lepton

$$\mu_\nu = \frac{3\,e\,G_F}{8\sqrt{2}\,\pi^2} m_\nu \simeq 3.2 \times 10^{-19} \left(\frac{m_\nu}{\mathrm{eV}}\right) \mu_B$$

The electromagnetic vertex allows for the presence of electric and magnetic dipole

The magnetic moment interaction adds incoherently to the weak interaction because it flips helicity.

$$\frac{d\sigma_{\nu_\ell\text{-}\mathcal{N}}}{dT_{\mathrm{nr}}}(E, T_{\mathrm{nr}}) = \frac{d\sigma^{\mathrm{SM}}_{\nu_\ell\text{-}\mathcal{N}}}{dT_{\mathrm{nr}}}(E, T_{\mathrm{nr}}) + \frac{d\sigma^{\mathrm{mag}}_{\nu_\ell\text{-}\mathcal{N}}}{dT_{\mathrm{nr}}}(E, T_{\mathrm{nr}})$$

Measurement of Weinber angle

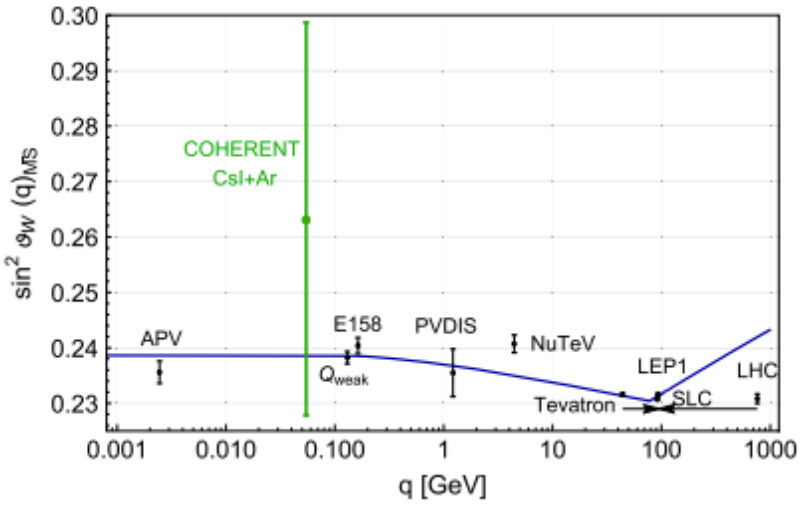

FIG. 4. Variation of $\sin^2\vartheta_W$ with energy scale q. The SM prediction is shown as the solid curve, together with experimental determinations in black at the Z pole [21] (Tevatron, LEP1, SLC, LHC), from APV on cesium [54,55], which has a typical momentum transfer given by $\langle q\rangle \simeq 2.4$ MeV, Møller scattering [56] (E158), deep inelastic scattering of polarized electrons on deuterons [57] (e^2H PVDIS), as well as from neutrino-nucleus scattering [58] (NuTeV) and the new result from the proton's weak charge at $q = 0.158$ GeV [59] (Q_{weak}). In green the result derived in this paper is shown, obtained fitting the Ar and CsI COHERENT dataset. For clarity we displayed the Tevatron and LHC points horizontally to the left and to the right, respectively.

Weak Mixing Angle

Theory: $\sin^2\vartheta_W = 0.23857 \pm 0.00005$

Our result

$$\sin^2\vartheta_W(\mathrm{Ar}) = 0.31 \pm 0.06\,(1\sigma), ^{+0.11}_{-0.13}\,(2\sigma), ^{+0.18}_{-0.23}\,(3\sigma)$$

$$\sin^2\vartheta_W(\mathrm{CsI}) = 0.24 \pm 0.04\,(1\sigma), \pm 0.09\,(2\sigma), ^{+0.13}_{-0.14}\,(3\sigma)$$

$$\sin^2\vartheta_W(\mathrm{CsI+Ar}) = 0.26^{+0.04}_{-0.03}\,(1\sigma), \pm 0.07\,(2\sigma), \pm 0.11\,(3\sigma)$$

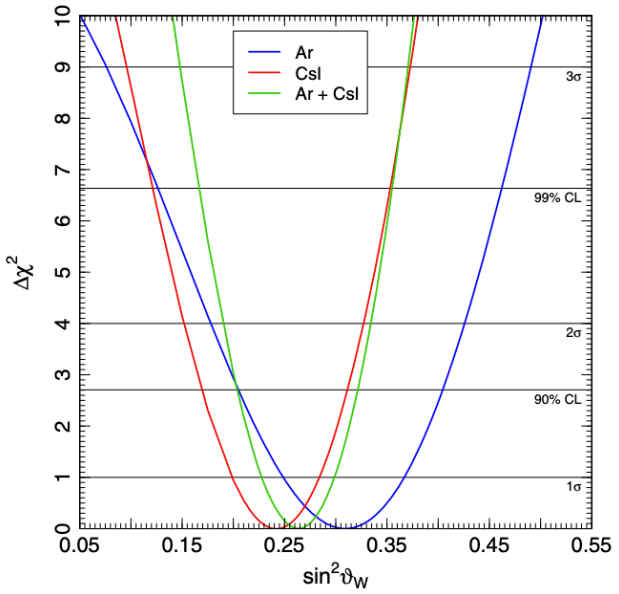

Neutrino charge radii

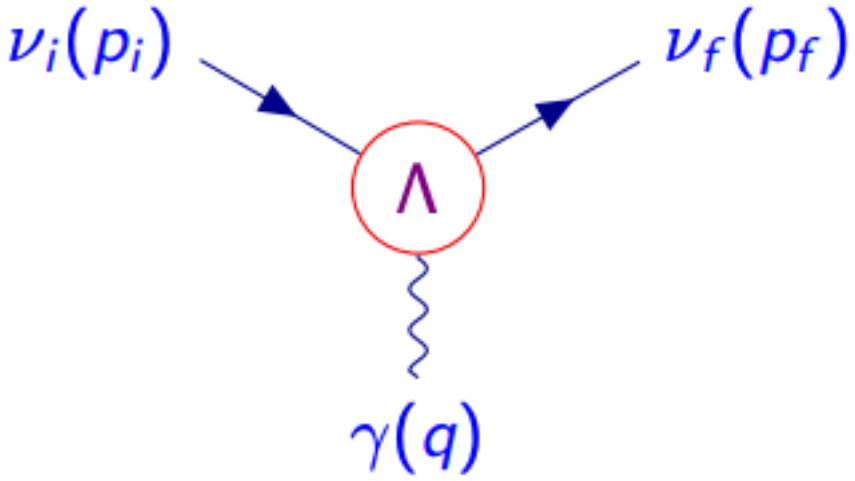

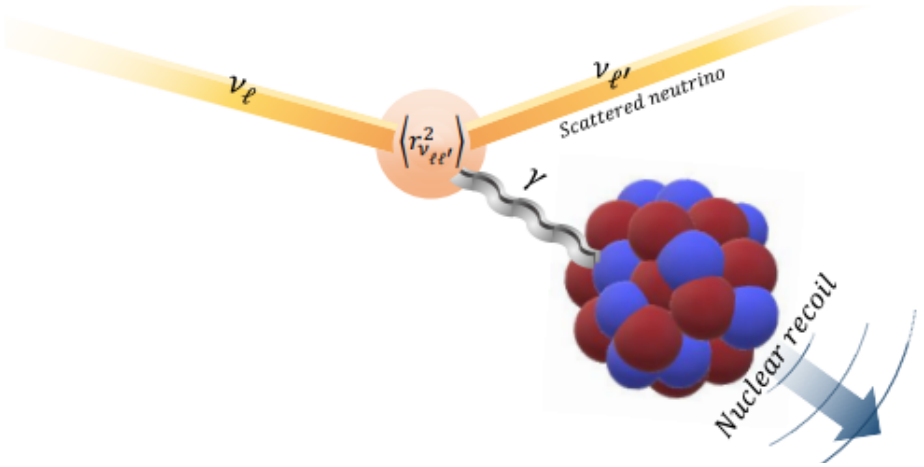

Effective Hamiltonian: $\mathcal{H}^{(\nu)}_{\rm em}(x) = j^{(\nu)}_\mu(x) A^\mu(x) = \sum_{k,j=1} \overline{\nu_k}(x) \Lambda^{kj}_\mu \nu_j(x) A^\mu(x)$

Radiative corrections generate an effective electromagnetic interaction vertex

$\Lambda_\mu(q) = \left(\gamma_\mu - q_\mu \not{q}/q^2\right) F(q^2)$

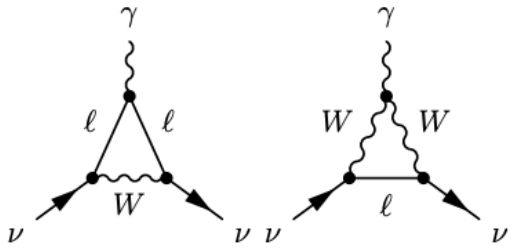

In the Standard Model there are only diagonal charge radii $\langle r^2_{\nu_\ell} \rangle \equiv \langle r^2_{\nu_{\ell\ell}} \rangle$ because lepton numbers are conserved.

Radiative correction

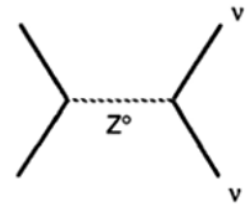

"Tree Level"

$$\frac{1}{2} - 2\sin^2\vartheta_W$$

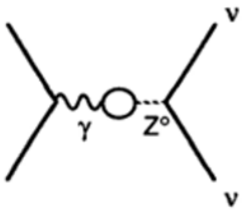

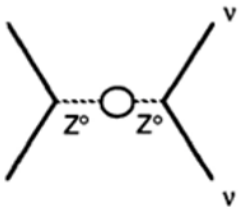

γ - Z° Mixing & Self-Energies

$$\rho\left(\frac{1}{2} - 2\sin^2\vartheta_W\right)$$

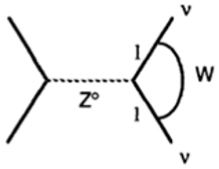

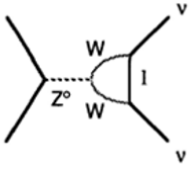

Vertex

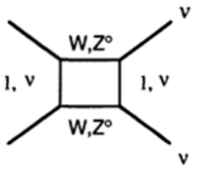

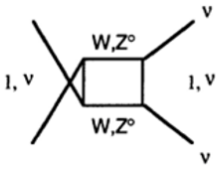

Box Diagrams

$$\frac{\hat{\alpha}_Z}{4\pi\hat{s}_Z^2}\left(1 - 2\,\frac{\hat{\alpha}_s(m_W)}{\pi}\right)$$

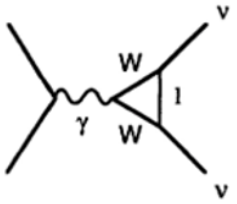

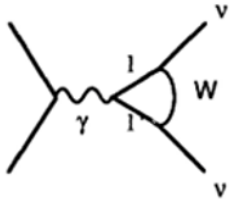

Charge Radius

$$\frac{\alpha}{6\pi}\left(3 - 2\ln\frac{m_\ell^2}{m_W^2}\right)$$

CEvNS cross section at loop-level

$$\frac{d\sigma_{\nu_\ell - \mathcal{N}}}{dT_{\rm nr}}(E, T_{\rm nr})$$

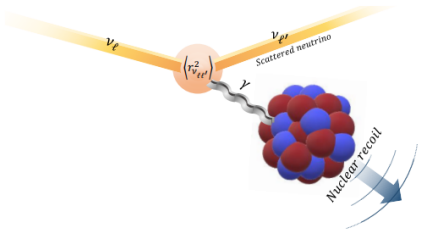

$$= \frac{G_{\rm F}^2 M}{\pi}\left(1 - \frac{MT_{\rm nr}}{2E^2}\right)\left[g_V^p Z F_Z(|\vec{q}|^2) + g_V^n N F_N(|\vec{q}|^2)\right]^2$$

Tree-level values

$$g_V^p = \frac{1}{2} - 2\sin^2\vartheta_W, \qquad g_V^n = -\frac{1}{2}$$

Taking into account radiative corretions

$$g_V^p(\nu_\ell) = \rho\left(\frac{1}{2} - 2\sin^2\vartheta_W\right) - \frac{\hat{\alpha}_Z}{4\pi\hat{s}_Z^2}\left(1 - 2\frac{\hat{\alpha}_s(m_W)}{\pi}\right) + \frac{\alpha}{6\pi}\left(3 - 2\ln\frac{m_\ell^2}{m_W^2}\right),$$

$$g_V^n = -\frac{\rho}{2} - \frac{\hat{\alpha}_Z}{8\pi\hat{s}_Z^2}\left(7 - 5\frac{\hat{\alpha}_s(m_W)}{\pi}\right),$$

$$g_V^p(\nu_e) = 0.0401,$$

$$g_V^p(\nu_\mu) = 0.0318,$$

$$g_V^n = -0.5094.$$

Measurement of neutrino charge radii

Assuming non diagonal terms

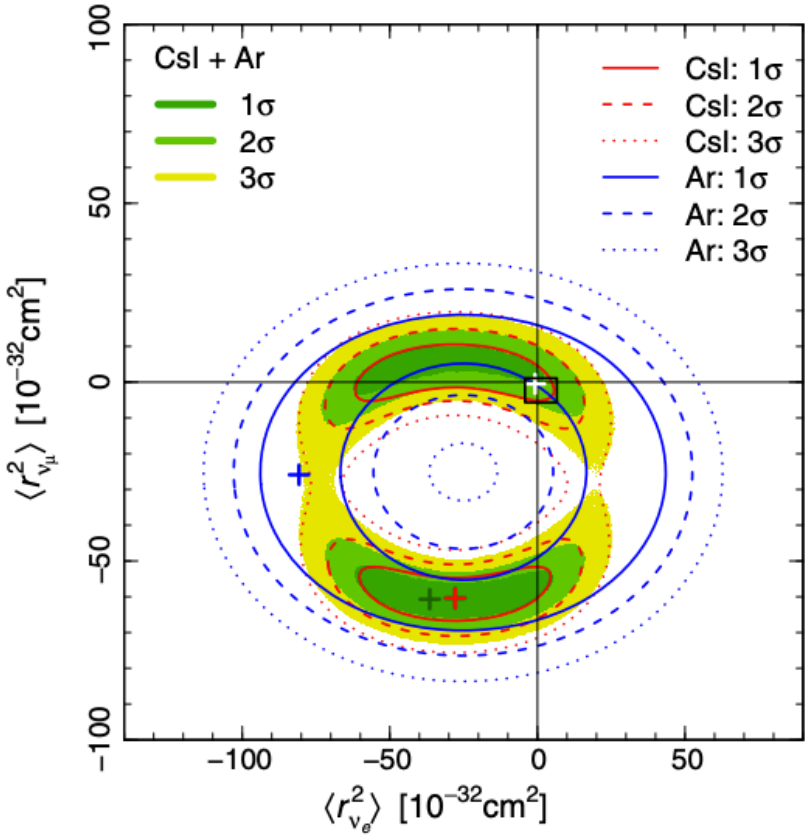

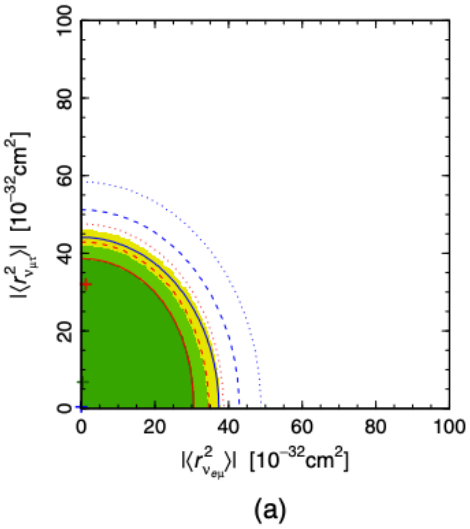

(a)

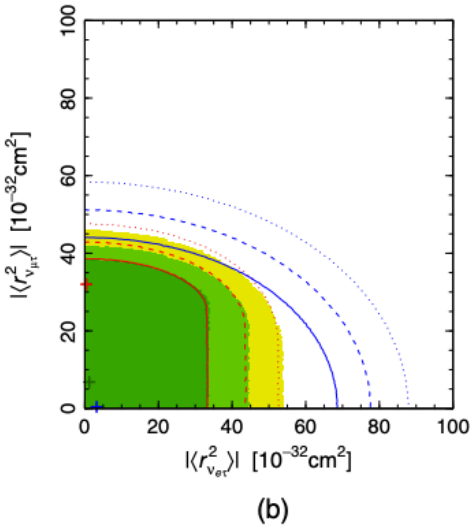

(b)

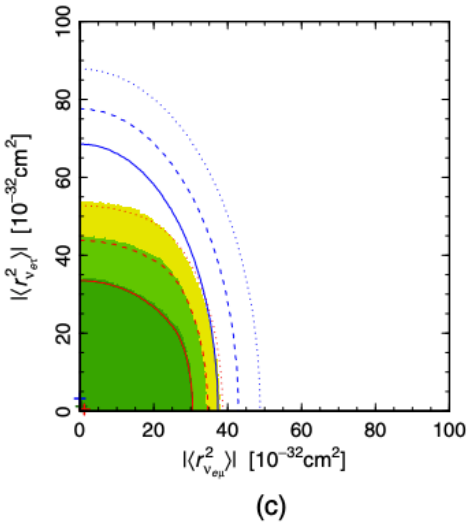

(c)

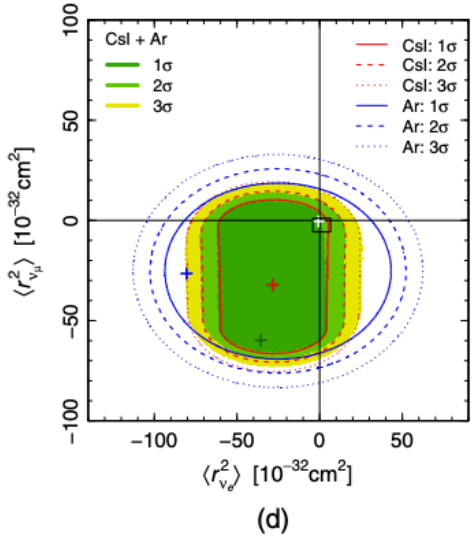

(d)

CENNS-10 detector

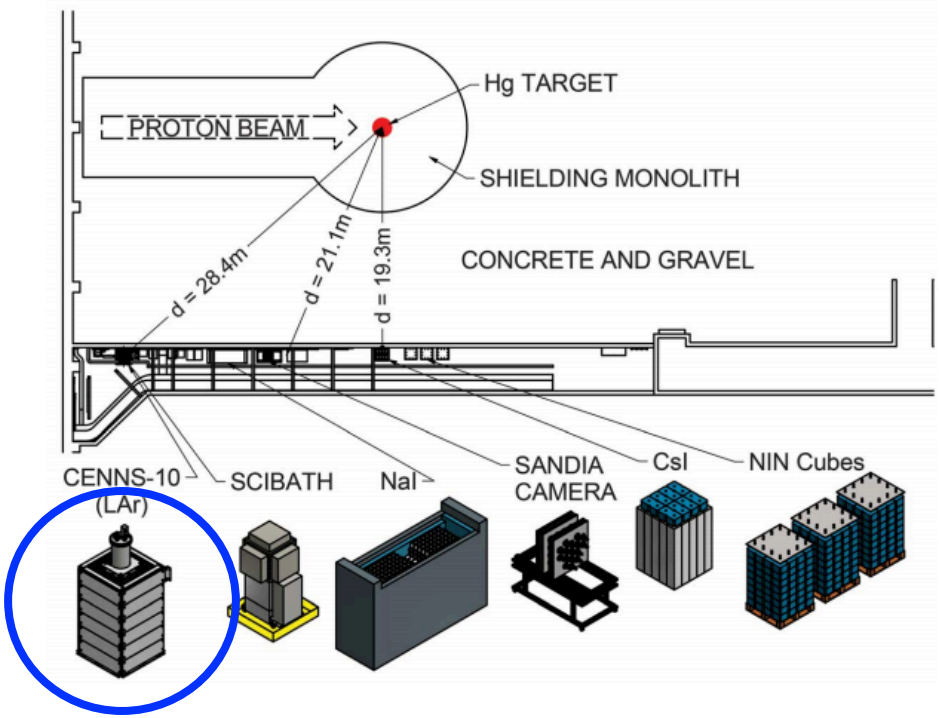

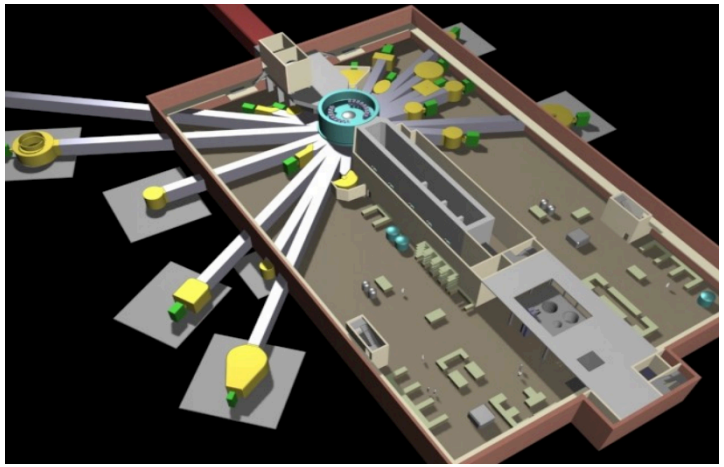

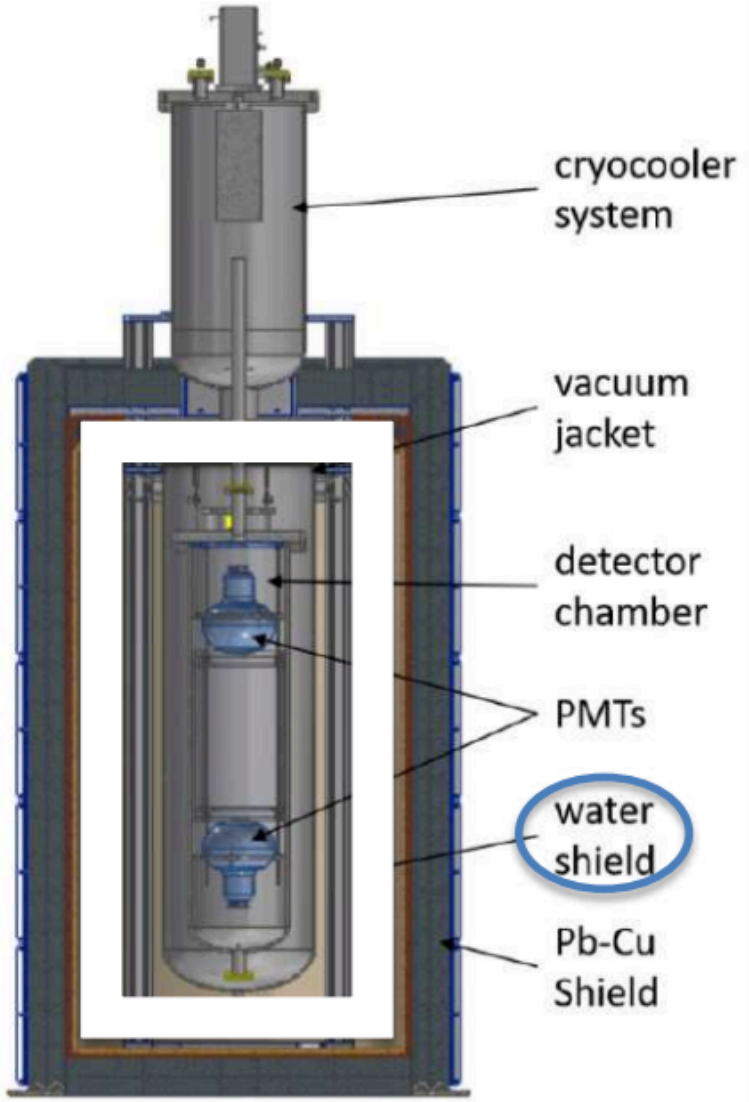

Z' contribution to the rate

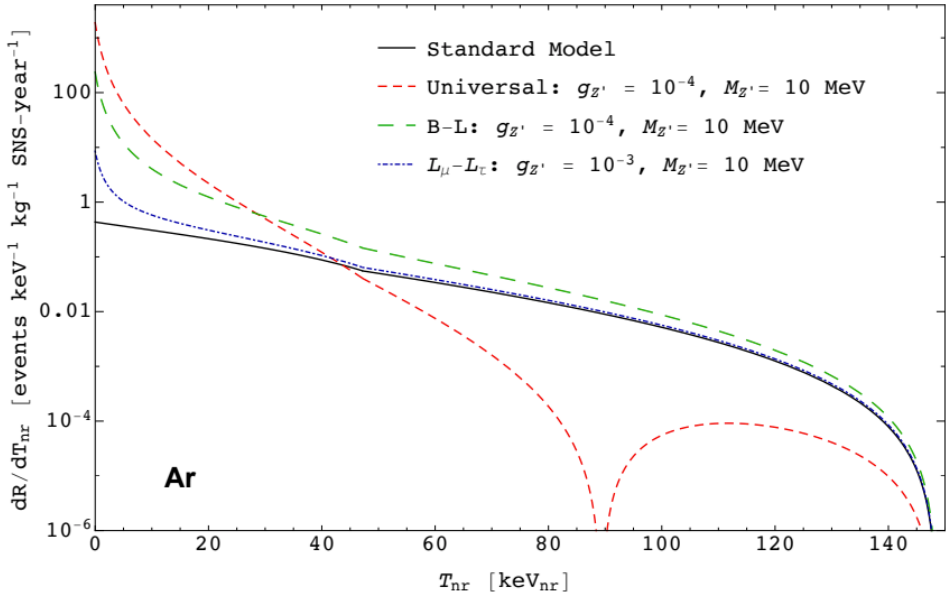

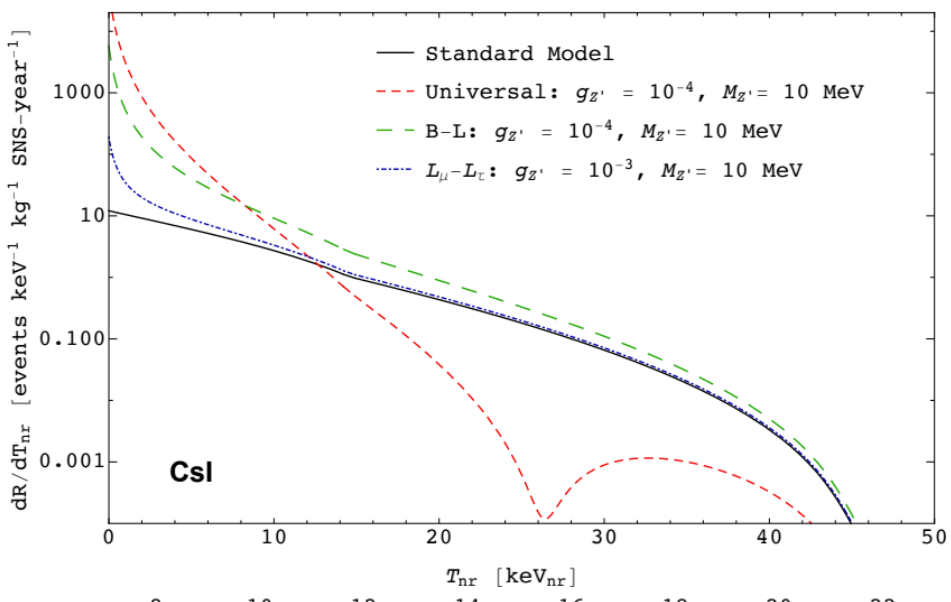

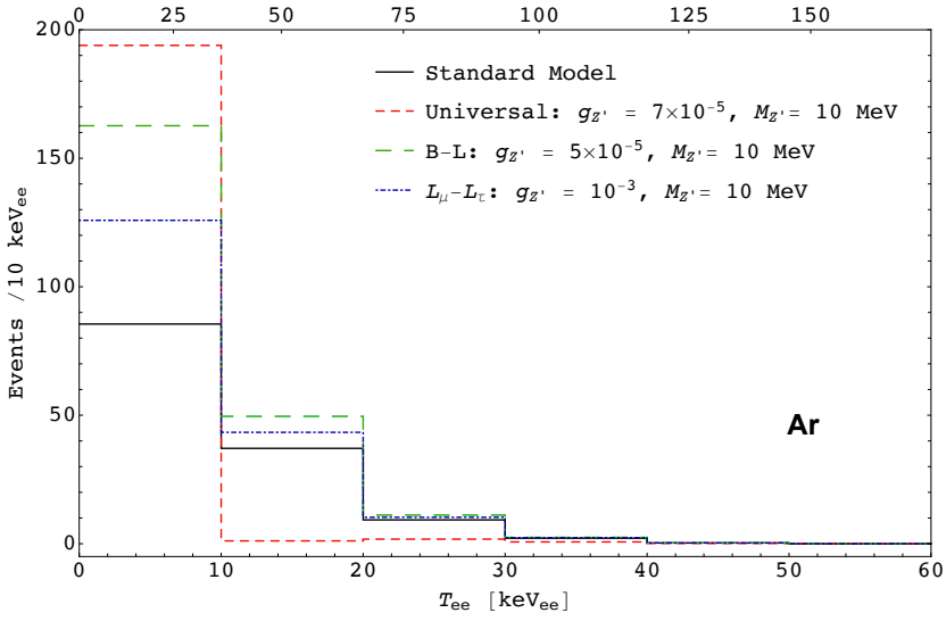

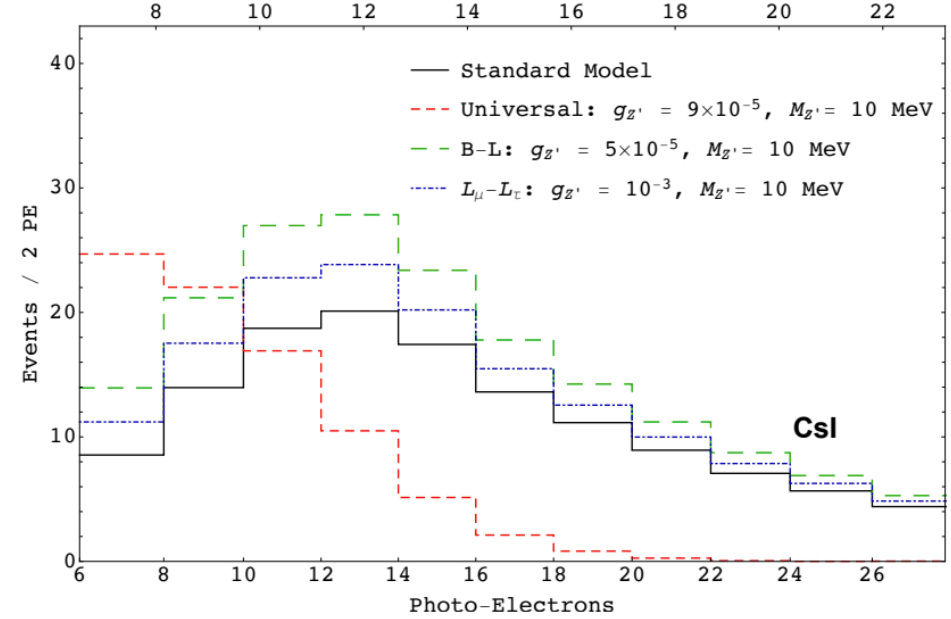

Constraints on Universal Model

$$\mathcal{L} = \mathcal{L}_{SM} - \frac{1}{4} Z'^{\mu\nu} Z'_{\mu\nu} + \frac{1}{2} M^2_{Z'} Z'^{\mu} Z'_{\mu} + Z'_{\mu} J^{\mu}_{X}$$

$$J^{\mu}_{X} = g' \Big[\sum_{q} Q'_q \bar{q} \gamma^{\mu} q + \sum_{L_l = \nu_{lL}, l} Q'_l \bar{L}_l \gamma^{\mu} L_l \Big]$$

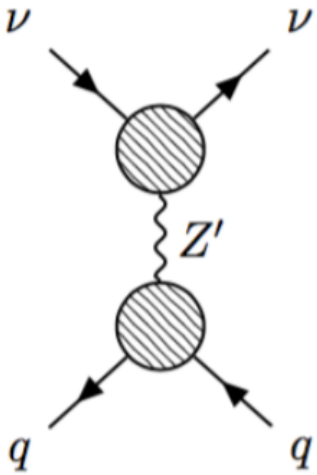

$$Q'_\ell \equiv Q'_f = 1,$$

Same coupling with all the fermions

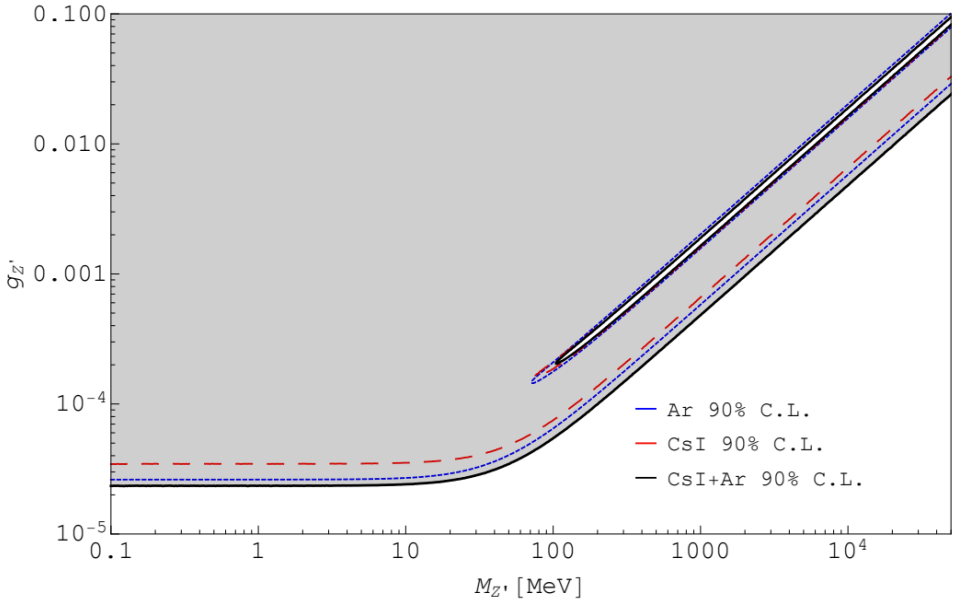

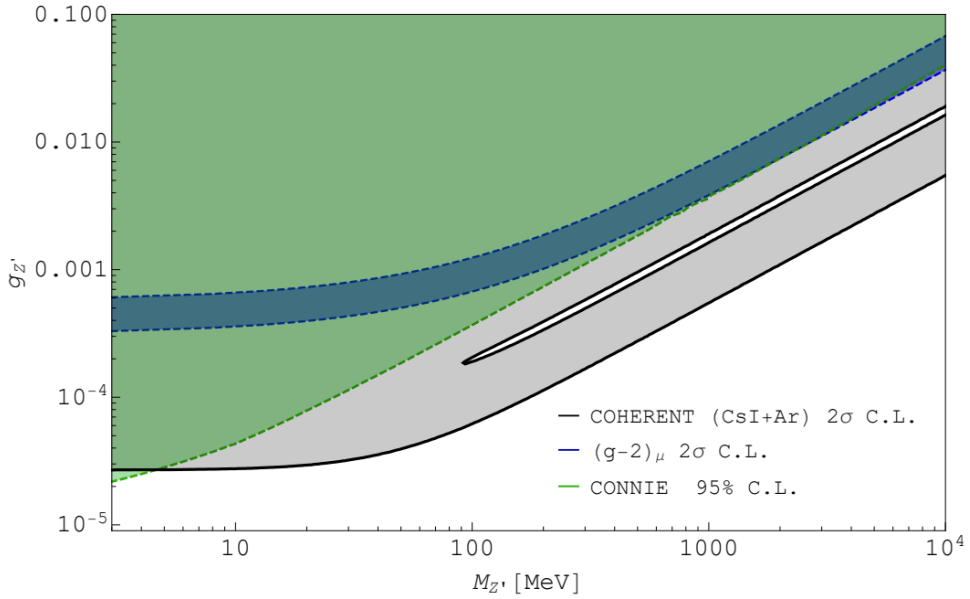

CONNIE collaboration - JHEP 04 (2020) 054
A. Drukier and L. Stodolsky - Phys. Rev. D30 (1984) 2295
J. Barranco, O. Miranda and T. Rashba - JHEP 12 (2005) 021

Constraints on B-L

The second model that we consider is the so-called $B - L$ (baryon number minus lepton number) extension of the SM [20, 21]. In this case the gauge charges are determined by imposing that the theory is anomaly free. In particular, in this model the boson couples universally to the quarks, as well as to the neutrinos, but with different charges, namely $Q'_\ell \neq Q'_f$. In particular, in the $B - L$ model the gauge charges are such that $Q'_\ell = 1$ and $Q'_f = -Q'_\ell/3$.

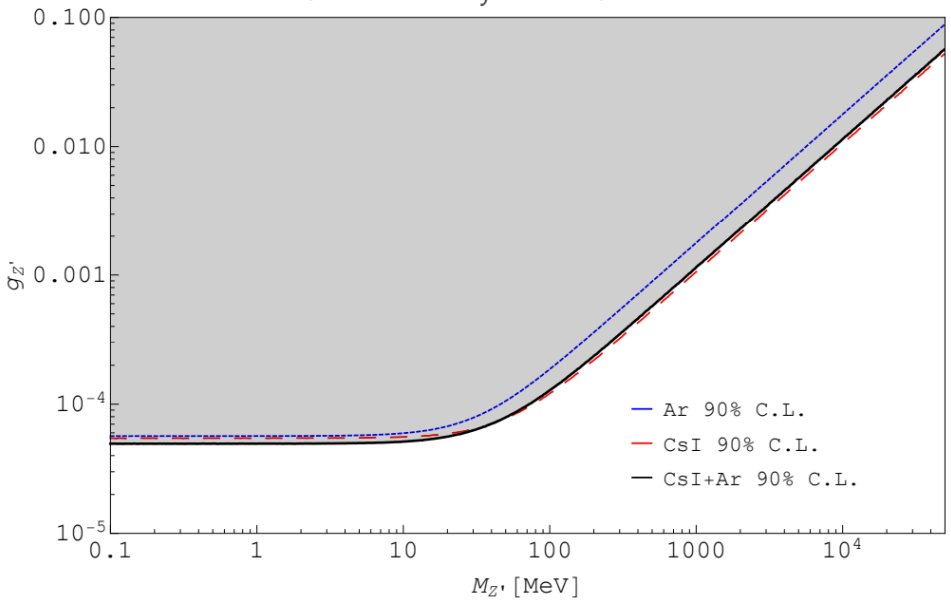

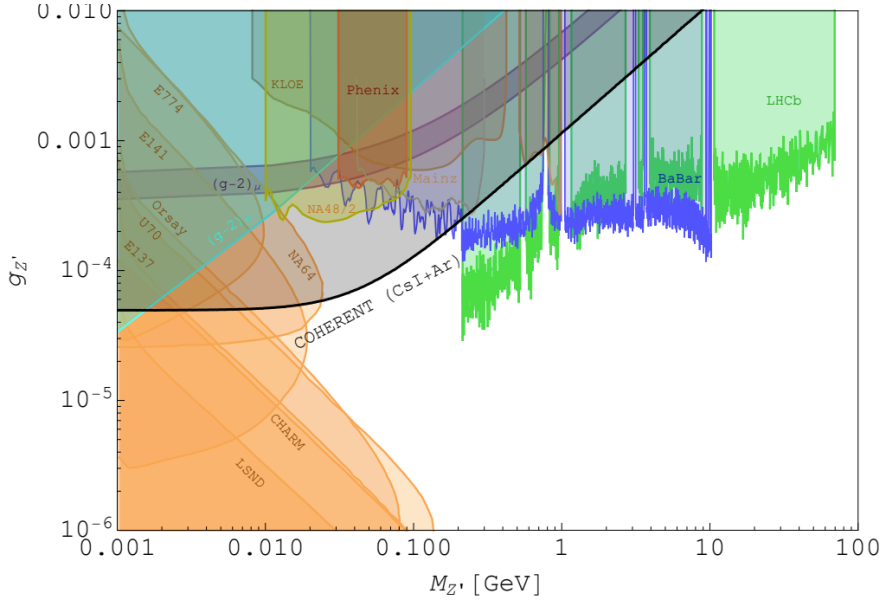

BaBar collaboration, Phys. Rev. Lett. 113 (2014) 201801
LHCb collaboration, Phys. Rev. Lett. 124 (2020) 041801
PHENIX Collaboration - Phys. Rev. C 91 (2015) 031901
ALICE collaboration - Phys. Lett. B 720 (2013) 52
NA48/2 collaboration - Phys. Lett. B 746 (2015) 178
A1 Collaboration collaboration - Phys. Rev. Lett. 106 (2011) 251802.
R. Harnik, J. Kopp and P.A. Machado - JCAP 07 (2012) 026
Muon g-2 collaboration -, Phys. Rev. D 73 (2006) 072003
H. Davoudiasl and W.J. Marciano - Phys. Rev. D 98 (2018) 075011

Constraints on Lμ-Lτ

$$\mathcal{L}_{int}^{\mu\tau} \supset g_{Z'} Q_{\alpha\beta} (\bar{l}_\alpha \gamma^\mu l_\beta + \bar{\nu}_{L\alpha} \gamma^\mu \nu_{L\beta}) Z'_\mu$$

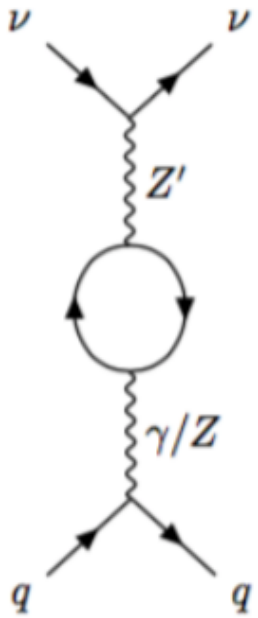

The last scenario that we consider is a model with gauged Lμ − Lτ symmetry. In this case, the new Z′ boson can couple directly only to muonic or tauonic flavour and there is no tree-level coupling to the quark sector. Thus, this model can be studied through the CEνNS process by considering the interaction between the new boson and quarks via kinetic loops of muons and tauons involving photons

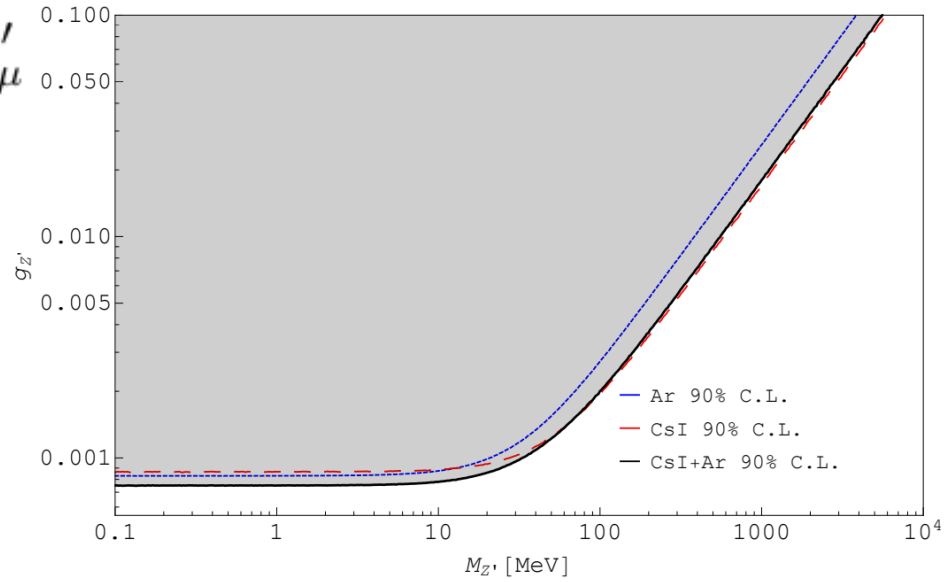

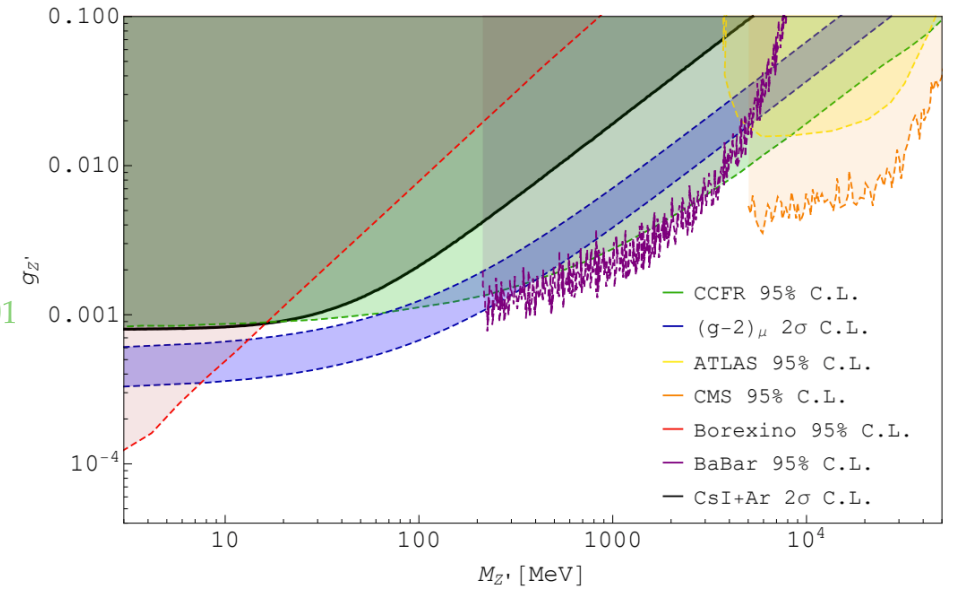

W. Altmannshofer et al. - Phys. Rev. Lett. 113 (2014) 091801
ATLAS collaboration - Phys. Rev. Lett. 112 (2014) 231806
CMS collaboration-Phys. Lett. B 792 (2019) 345
BaBar collaboration - Phys. Rev. D 94 (2016) 011102
S. Gninenko and D. Gorbunov - arXiv:2007.16098
Muon g-2 collaboration -, Phys. Rev. D 73 (2006) 072003